NSTX

Supported by

U.S. DEPARTMENT OF ENERGY

Office of Science

The Role of Kinetic Effects, Including Fast Particles, in Resistive Wall Mode Stability

Jack Berkery

Department of Applied Physics, Columbia University, New York, NY, USA

College W&M
Colorado Sch Mines
Columbia U
CompX
General Atomics
INEL
Johns Hopkins U
LANL
LLNL
Lodestar
MIT
Nova Photonics
New York U
Old Dominion U
ORNL
PPPL
PSI
Princeton U
Purdue U
SNL
Think Tank, Inc.
UC Davis
UC Irvine
UCLA
UCSD
U Colorado
U Illinois
U Maryland
U Rochester
U Washington
U Wisconsin

51st Annual Meeting of the Division of Plasma Physics
Atlanta, Georgia
November 3, 2009

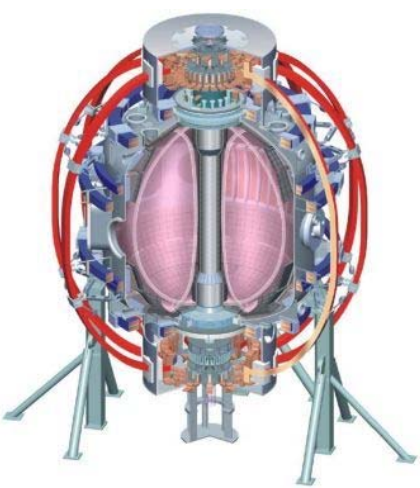

Culham Sci Ctr
U St. Andrews
York U
Chubu U
Fukui U
Hiroshima U
Hyogo U
Kyoto U
Kyushu U
Kyushu Tokai U
NIFS
Niigata U
U Tokyo
JAEA
Hebrew U
Ioffe Inst
RRC Kurchatov Inst
TRINITI
KBSI
KAIST
POSTECH
ASIPP
ENEA, Frascati
CEA, Cadarache
IPP, Jülich
IPP, Garching
ASCR, Czech Rep
U Quebec

NSTX

Supported by

U.S. DEPARTMENT OF ENERGY | Office of Science

In collaboration with:

S.A. Sabbagh, H. Reimerdes

Department of Applied Physics, Columbia University, New York, NY, USA

R. Betti, B. Hu

Laboratory for Laser Energetics, University of Rochester, Rochester, NY, USA

R.E. Bell, S.P. Gerhardt, N. Gorelenkov,
J. Manickam, M. Podesta, R. White

Princeton Plasma Physics Laboratory, Princeton University, Princeton, NJ, USA

K. Tritz

Dept. of Physics and Astronomy, Johns Hopkins University, Baltimore, MD, USA

… and the NSTX team

Supported by:

U.S. Department of Energy Contracts
DE-FG02-99ER54524, DE-AC02-09CH11466, and DE-FG02-93ER54215

College W&M
Colorado Sch Mines
Columbia U
CompX
General Atomics
INEL
Johns Hopkins U
LANL
LLNL
Lodestar
MIT
Nova Photonics
New York U
Old Dominion U
ORNL
PPPL
PSI
Princeton U
Purdue U
SNL
Think Tank, Inc.
UC Davis
UC Irvine
UCLA
UCSD
U Colorado
U Illinois
U Maryland
U Rochester
U Washington
U Wisconsin

Culham Sci Ctr
U St. Andrews
York U
Chubu U
Fukui U
Hiroshima U
Hyogo U
Kyoto U
Kyushu U
Kyushu Tokai U
NIFS
Niigata U
U Tokyo
JAEA
Hebrew U
Ioffe Inst
RRC Kurchatov Inst
TRINITI
KBSI
KAIST
POSTECH
ASIPP
ENEA, Frascati
CEA, Cadarache
IPP, Jülich
IPP, Garching
ASCR, Czech Rep
U Quebec

Stabilization from kinetic effects has the potential to explain experimental resistive wall mode (RWM) stability

- The RWM limits plasma pressure and leads to disruptions.
- Physics of RWM stabilization is key for extrapolation to:
  - sustained operation of a future NBI driven ST-CTF, and
  - disruption-free operation of a low rotation burning plasma (ITER).
- A kinetic theory is explored to explain experiments.
  - In NSTX, the RWM can go unstable with a wide range of rotation.
  - Stable discharges can have very low ω_ϕ (NSTX braking, DIII-D balanced beam).
  - Simple "critical rotation" model is insufficient.

A theoretical model broad enough in scope to explain these results is needed.

Outline

1. RWM experimental characteristics
2. Kinetic RWM stabilization theory: window of ω_ϕ with weakened stability
3. Comparison of theory and NSTX experimental results
4. The role of energetic particles

The RWM is identified in NSTX by a variety of observations

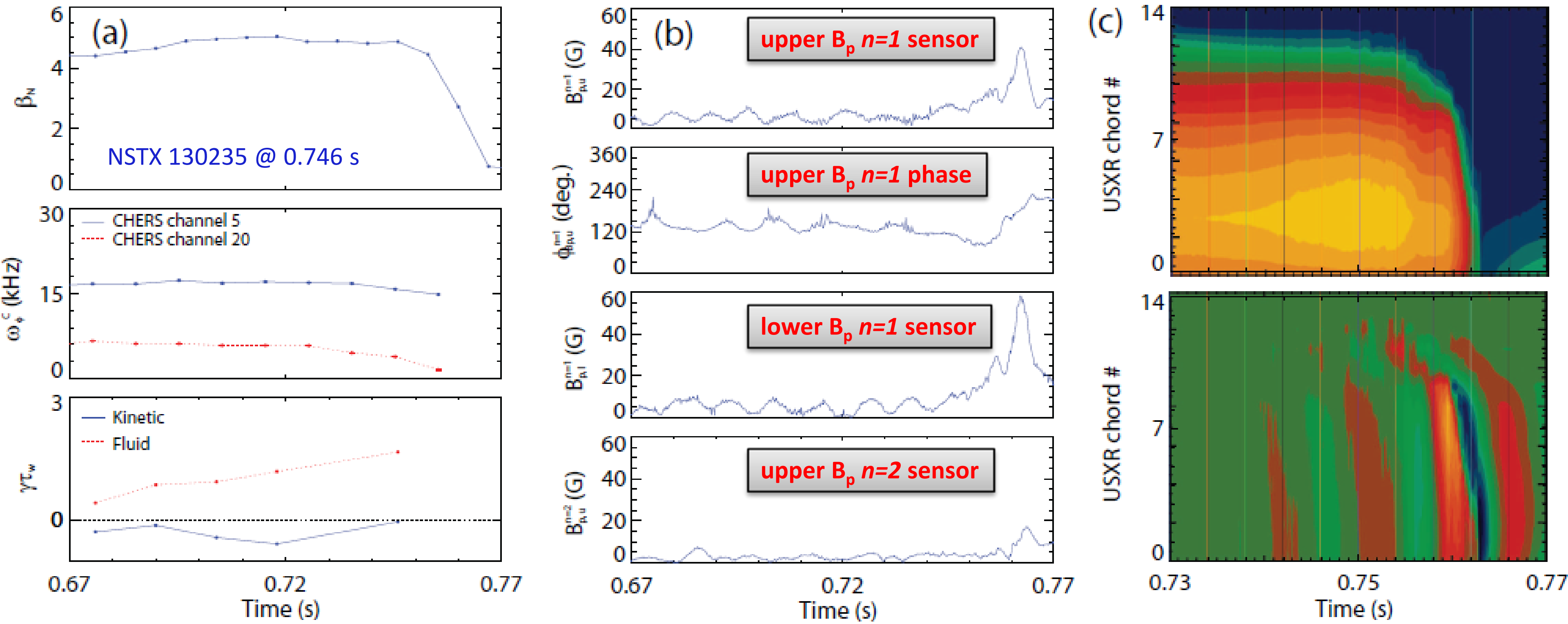

- Change in plasma rotation frequency, ω_ϕ
- Growing signal on low frequency poloidal magnetic sensors
- Global collapse in USXR signals, with no clear phase inversion
- Causes a collapse in β and disruption of the plasma

NSTX experimental results can not be explained with simple theories, but can potentially be explained by kinetic theory

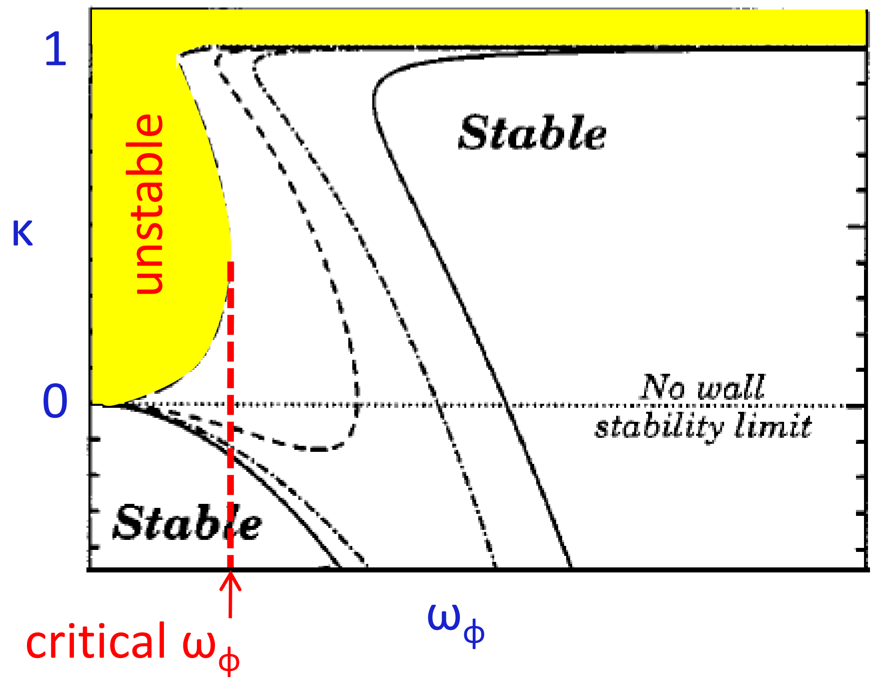

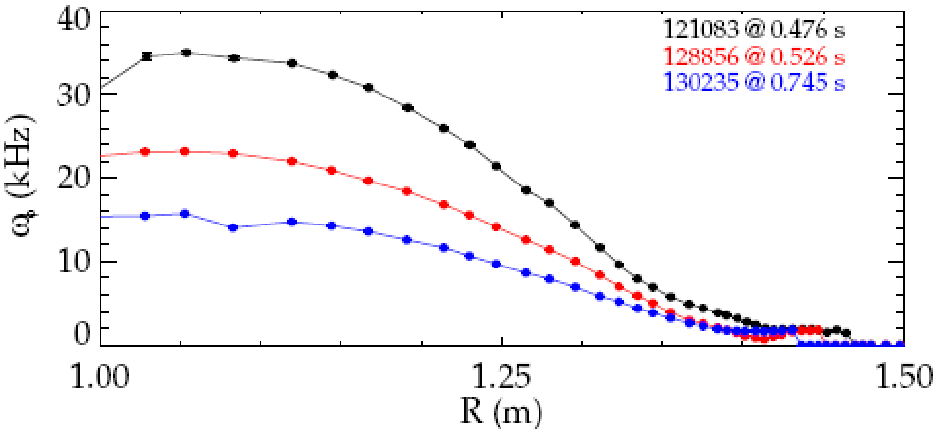

wide range of marginal profiles

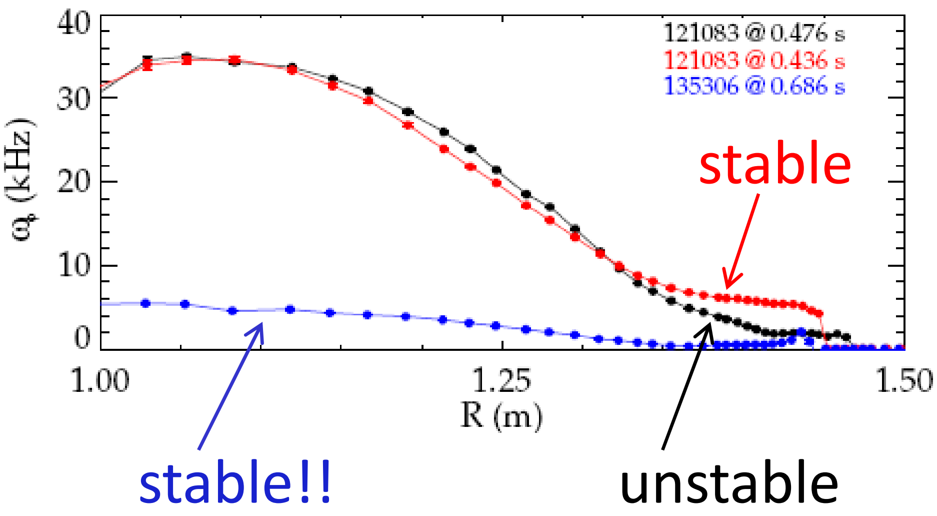

- Simple theories: "critical" rotation
- Kinetic theory can potentially explain NSTX experimental results

Kinetic δW_K term in the RWM dispersion relation provides dissipation that enables stabilization

Ideal theory alone shows instability above the no-wall limit:

$$\gamma\tau_w = -\frac{\delta W_\infty}{\delta W_b}$$

Dissipation enables stabilization:

$$(\gamma - i\omega_r)\tau_w = -\frac{\underset{\text{PEST}}{\delta W_\infty} + \underset{\text{MISK}}{\delta W_K}}{\delta W_b + \delta W_K}$$

PEST MISK

(Hu, Betti, and Manickam, PoP, 2005)

- Perturbative calculation of δW_K includes:
  - Trapped Ions and Electrons
  - Circulating Ions
  - Alfven Layers
  - Trapped Energetic Particles

Thermal Particles:

$$\delta W_K \sim \left[\frac{\omega_{*N} + \left(\hat{\varepsilon} - \frac{3}{2}\right)\omega_{*T} + \omega_E - \omega_r - i\gamma}{\underbrace{\langle\omega_D\rangle}_{\text{precession drift}} + \underbrace{l\omega_b}_{\text{bounce}} - \underbrace{i\nu_{\text{eff}}}_{\text{collisionality}} + \omega_E - \omega_r - i\gamma}\right]$$

precession drift bounce collisionality

A window of weakened stability can be found between the bounce and precession drift stabilizing resonances

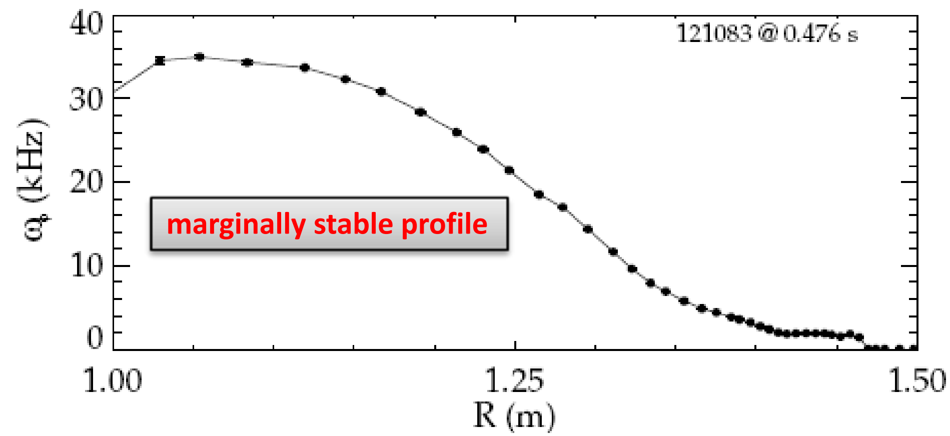

$$\delta W_K \sim \left[\frac{\omega_{*N} + \left(\hat{\varepsilon} - \frac{3}{2}\right)\omega_{*T} + \omega_E - \omega_r - i\gamma}{\langle\omega_D\rangle + l\omega_b - i\nu_{\text{eff}} + \omega_E - \omega_r - i\gamma} \right]$$

$$\omega_E = \omega_\phi - \omega_{*i}$$

- What causes this rotation profile to be marginally stable to the RWM?
  - Examine its relation to bounce and precession drift frequencies.

A window of weakened stability can be found between the bounce and precession drift stabilizing resonances

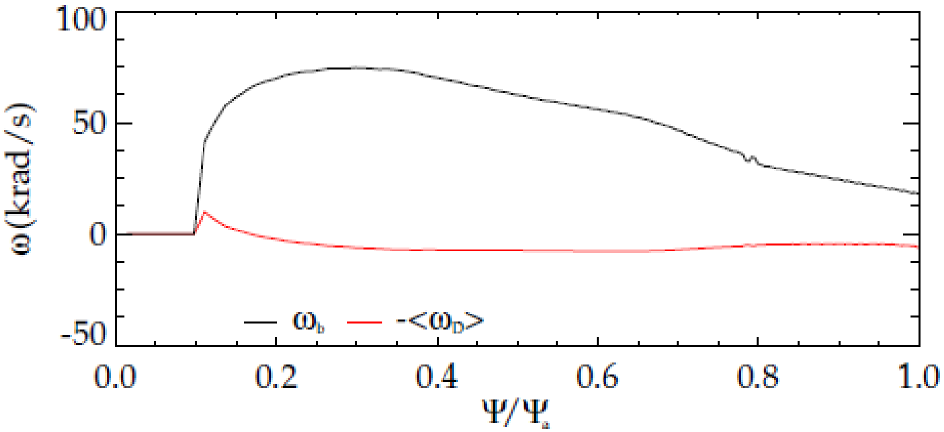

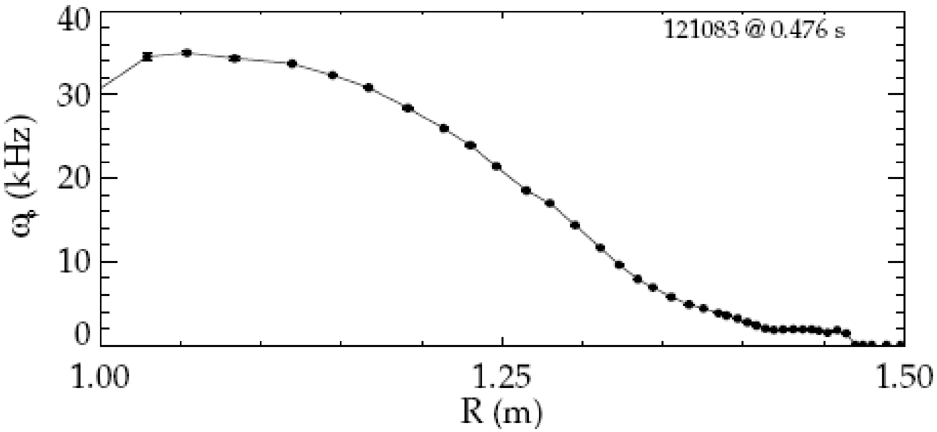

$$\delta W_K \sim \left[\frac{\omega_{*N} + \left(\hat{\varepsilon} - \frac{3}{2}\right)\omega_{*T} + \omega_E - \omega_r - i\gamma}{\langle\omega_D\rangle + l\omega_b - i\nu_{\text{eff}} + \omega_E - \omega_r - i\gamma} \right]$$

$$\omega_E = \omega_\phi - \omega_{*i}$$

- Resonance with bounce frequency: $\omega_E \approx \omega_b$
  - l=-1 harmonic
- Resonance with precession drift frequency: $\omega_E \approx -\langle\omega_D\rangle$

A window of weakened stability can be found between the bounce and precession drift stabilizing resonances

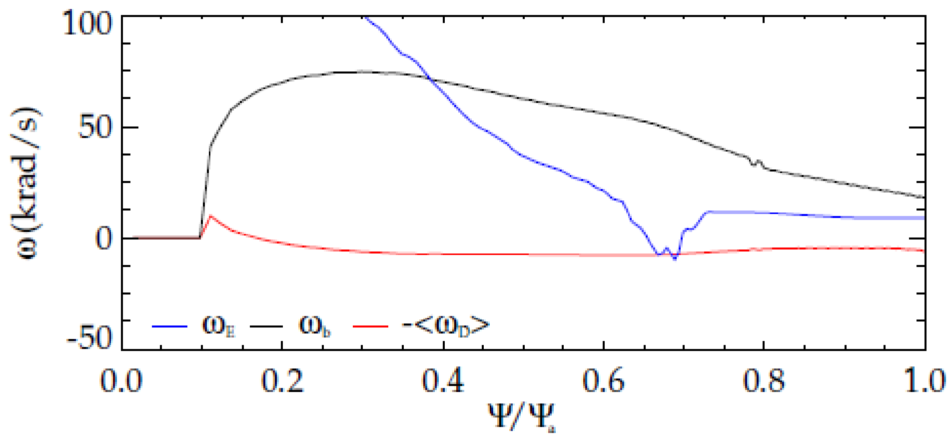

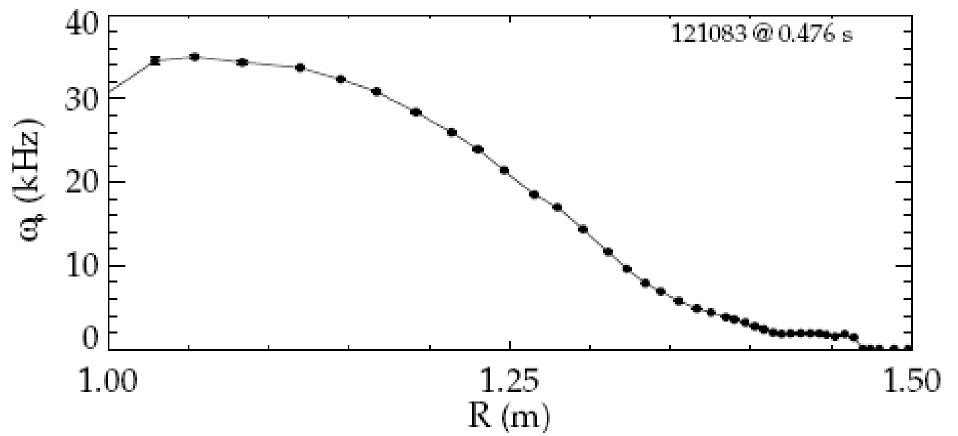

$$\delta W_K \sim \left[\frac{\omega_{*N} + \left(\hat{\varepsilon} - \frac{3}{2}\right)\omega_{*T} + \omega_E - \omega_r - i\gamma}{\langle\omega_D\rangle + l\omega_b - i\nu_{\text{eff}} + \omega_E - \omega_r - i\gamma} \right]$$

$$\omega_E = \omega_\phi - \omega_{*i}$$

- The experimentally marginally stable ω_E profile is in-between the stabilizing resonances.

A window of weakened stability can be found between the bounce and precession drift stabilizing resonances

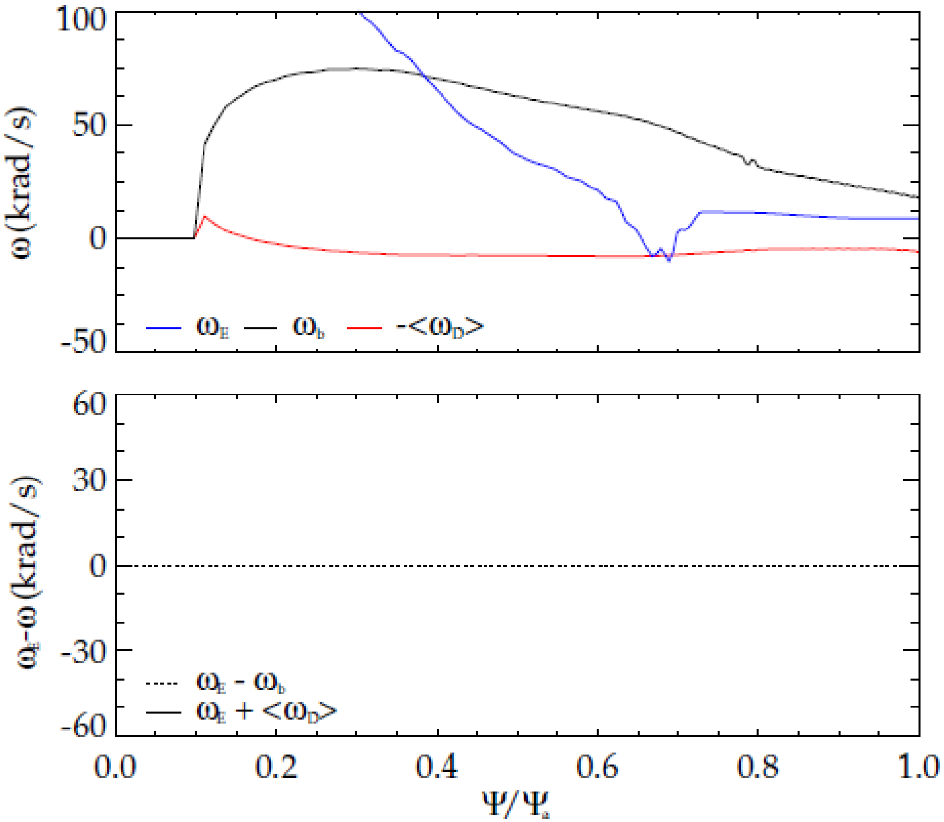

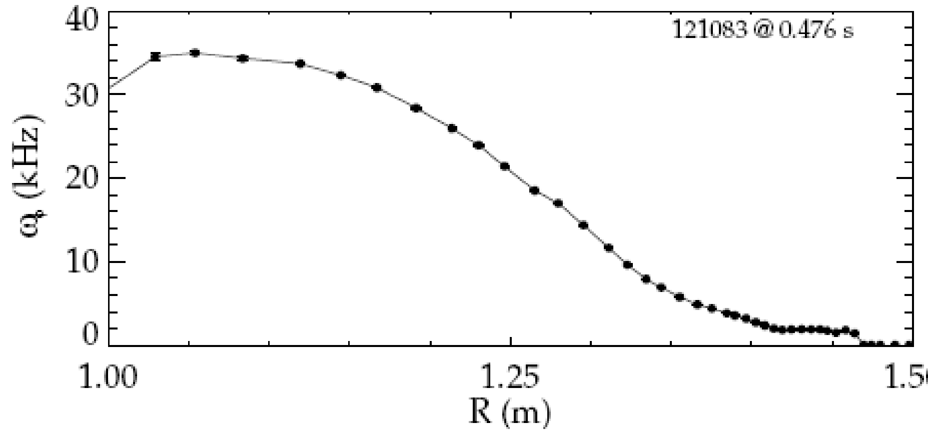

$$\delta W_K \sim \left[\frac{\omega_{*N} + \left(\hat{\varepsilon} - \frac{3}{2}\right)\omega_{*T} + \omega_E - \omega_r - i\gamma}{\langle \omega_D \rangle + l\omega_b - i\nu_{\text{eff}} + \omega_E - \omega_r - i\gamma} \right]$$

$$\omega_E = \omega_\phi - \omega_{*i}$$

- The experimentally marginally stable ω_E profile is in-between the stabilizing resonances.

A window of weakened stability can be found between the bounce and precession drift stabilizing resonances

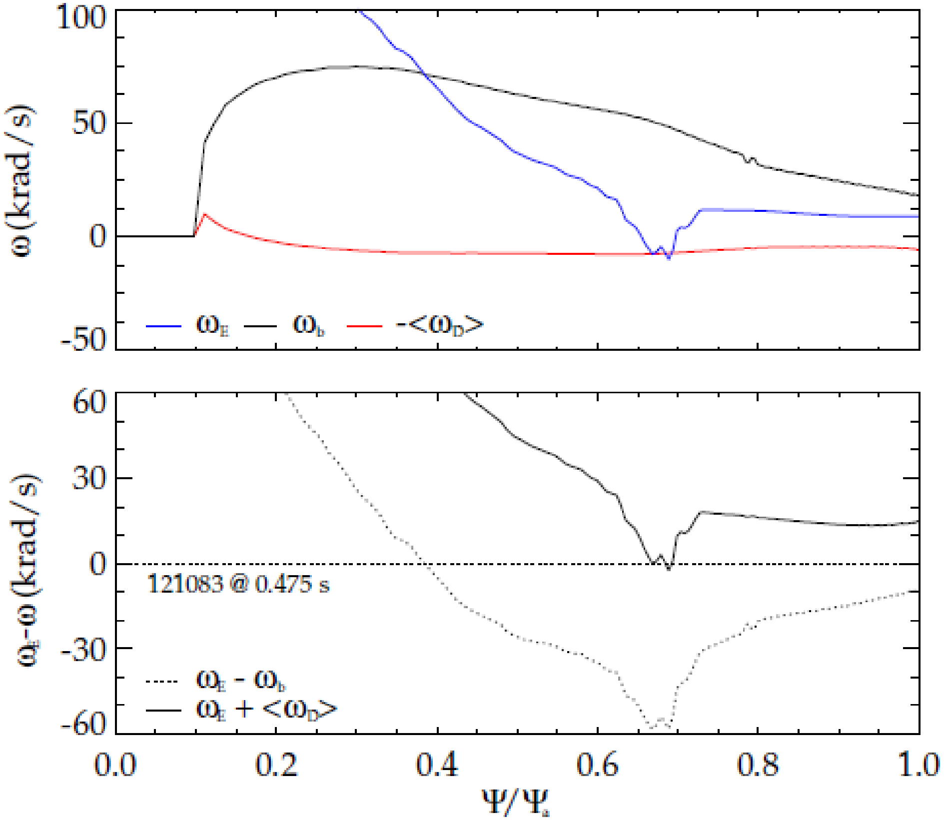

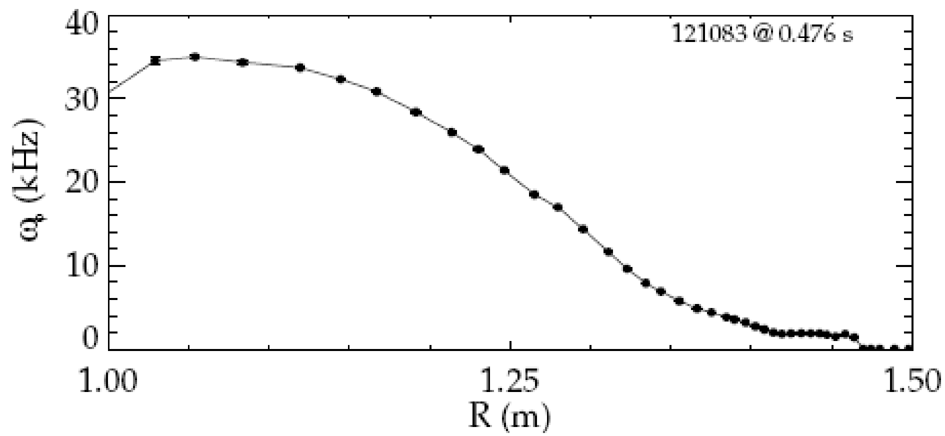

$$\delta W_K \sim \left[\frac{\omega_{*N} + \left(\hat{\varepsilon} - \frac{3}{2}\right)\omega_{*T} + \omega_E - \omega_r - i\gamma}{\langle \omega_D \rangle + l\omega_b - i\nu_{\mathrm{eff}} + \omega_E - \omega_r - i\gamma} \right]$$

$$\omega_E = \omega_\phi - \omega_{*i}$$

- The experimentally marginally stable ω_E profile is in-between the stabilizing resonances.

A window of weakened stability can be found between the bounce and precession drift stabilizing resonances

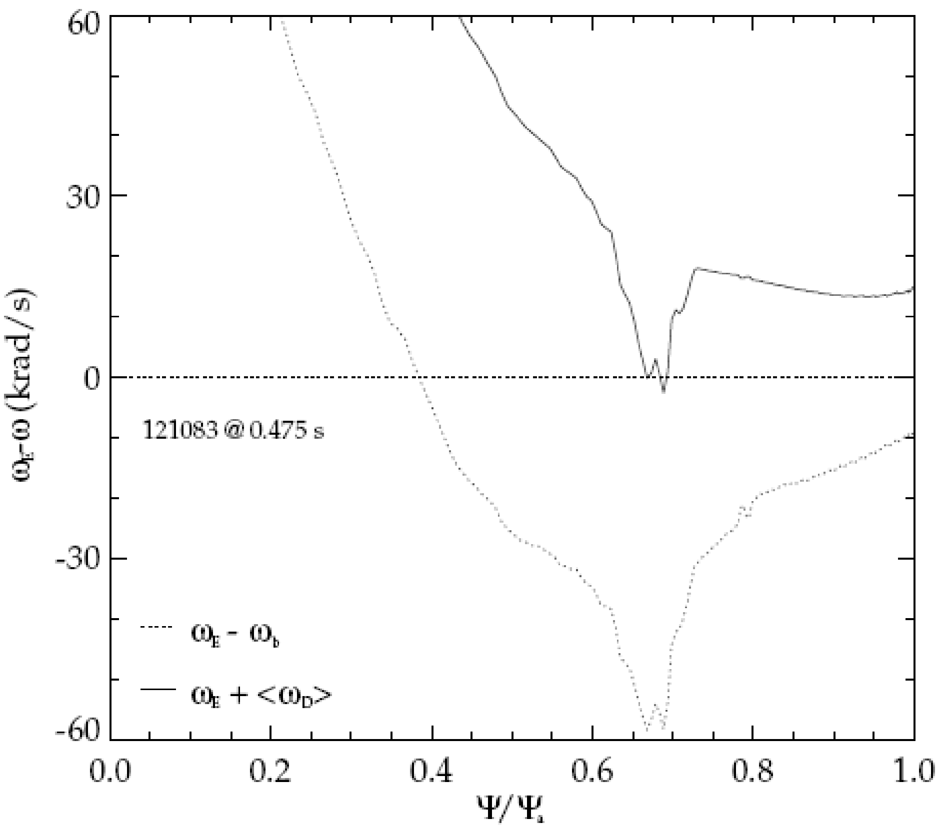

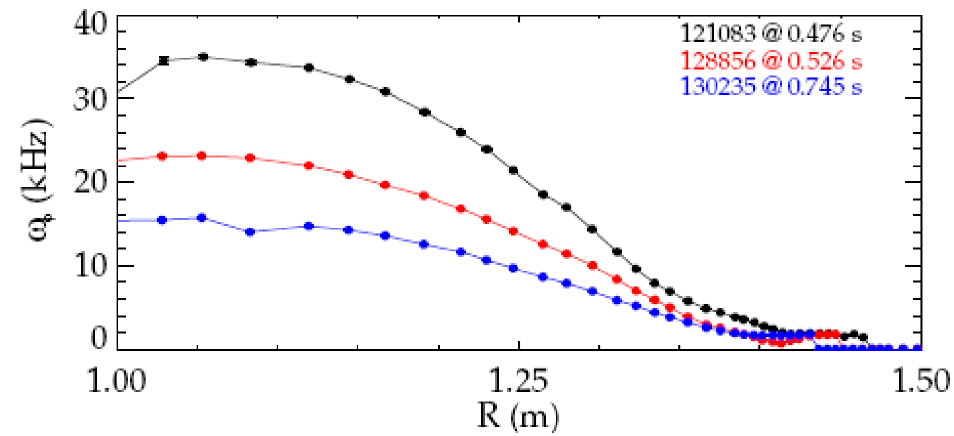

$$\delta W_K \sim \left[\frac{\omega_{*N} + \left(\hat{\varepsilon} - \frac{3}{2}\right)\omega_{*T} + \omega_E - \omega_r - i\gamma}{\langle \omega_D \rangle + l\omega_b - i\nu_{\text{eff}} + \omega_E - \omega_r - i\gamma} \right]$$

$$\omega_E = \omega_\phi - \omega_{*i}$$

- The experimentally marginally stable ω_E profile is in-between the stabilizing resonances.
  - Is this true for each of the widely different unstable profiles?

A window of weakened stability can be found between the bounce and precession drift stabilizing resonances

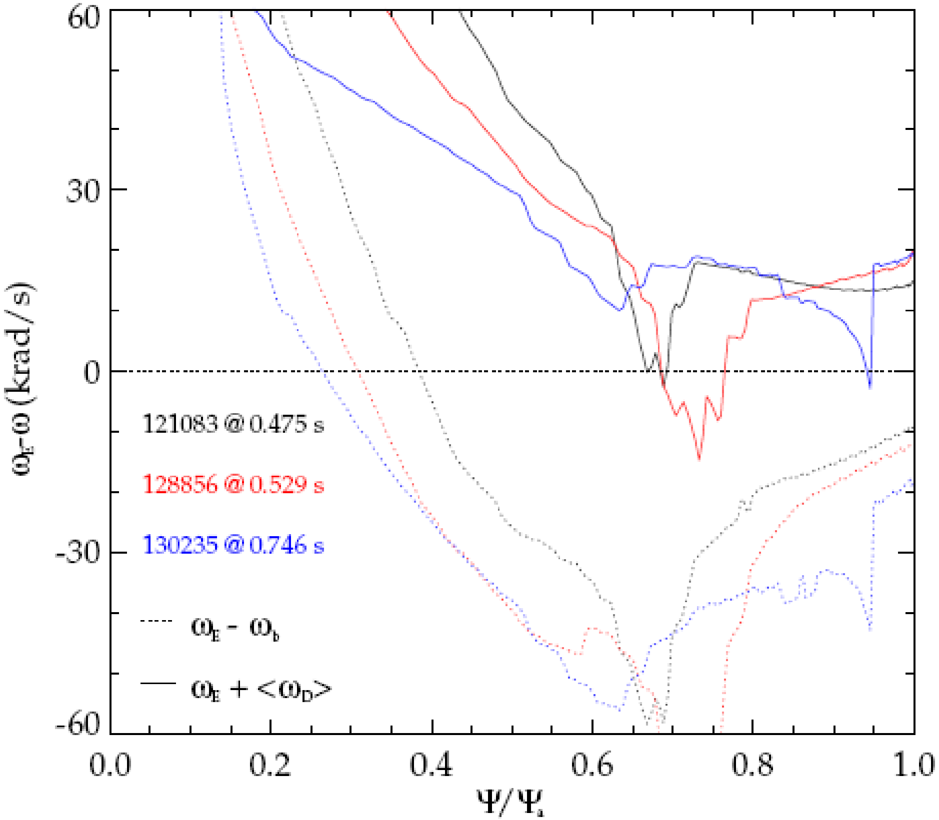

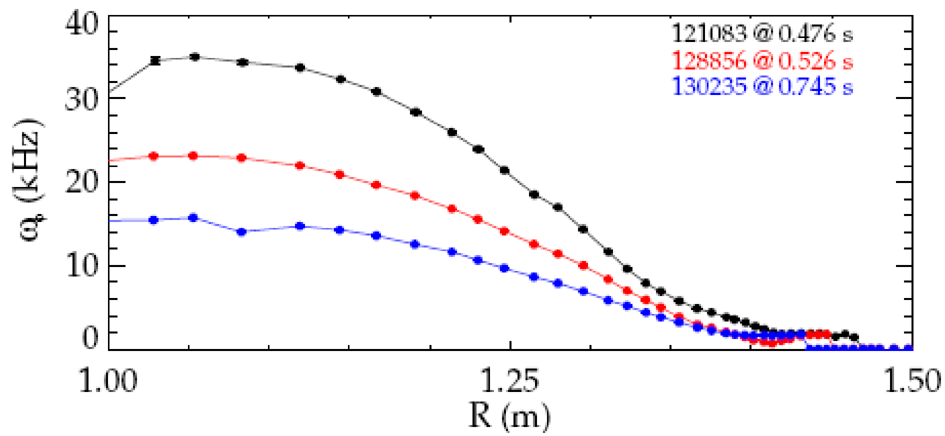

$$\delta W_K \sim \left[\frac{\omega_{*N} + \left(\hat{\varepsilon} - \frac{3}{2}\right)\omega_{*T} + \omega_E - \omega_r - i\gamma}{\langle\omega_D\rangle + l\omega_b - i\nu_{\mathrm{eff}} + \omega_E - \omega_r - i\gamma} \right]$$

$$\omega_E = \omega_\phi - \omega_{*i}$$

- The experimentally marginally stable ω_E profile is in-between the stabilizing resonances.
  - Is this true for each of the widely different unstable profiles: Yes

A window of weakened stability can be found between the bounce and precession drift stabilizing resonances

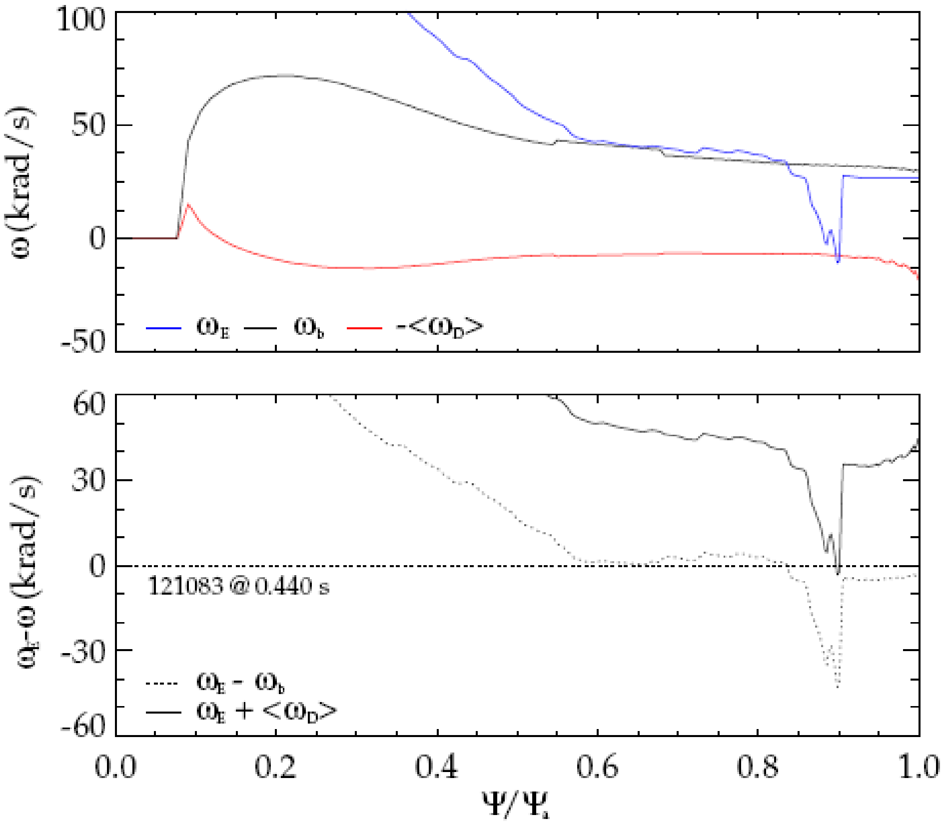

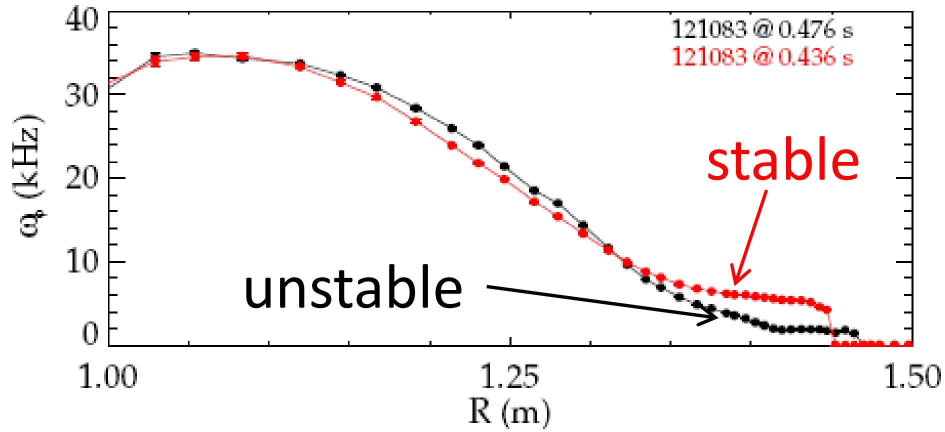

$$\delta W_K \sim \left[\frac{\omega_{*N} + \left(\hat{\varepsilon} - \frac{3}{2}\right)\omega_{*T} + \omega_E - \omega_r - i\gamma}{\langle \omega_D \rangle + l\omega_b - i\nu_{\text{eff}} + \omega_E - \omega_r - i\gamma} \right]$$

$$\omega_E = \omega_\phi - \omega_{*i}$$

- Stable cases in bounce resonance at “high” rotation

A window of weakened stability can be found between the bounce and precession drift stabilizing resonances

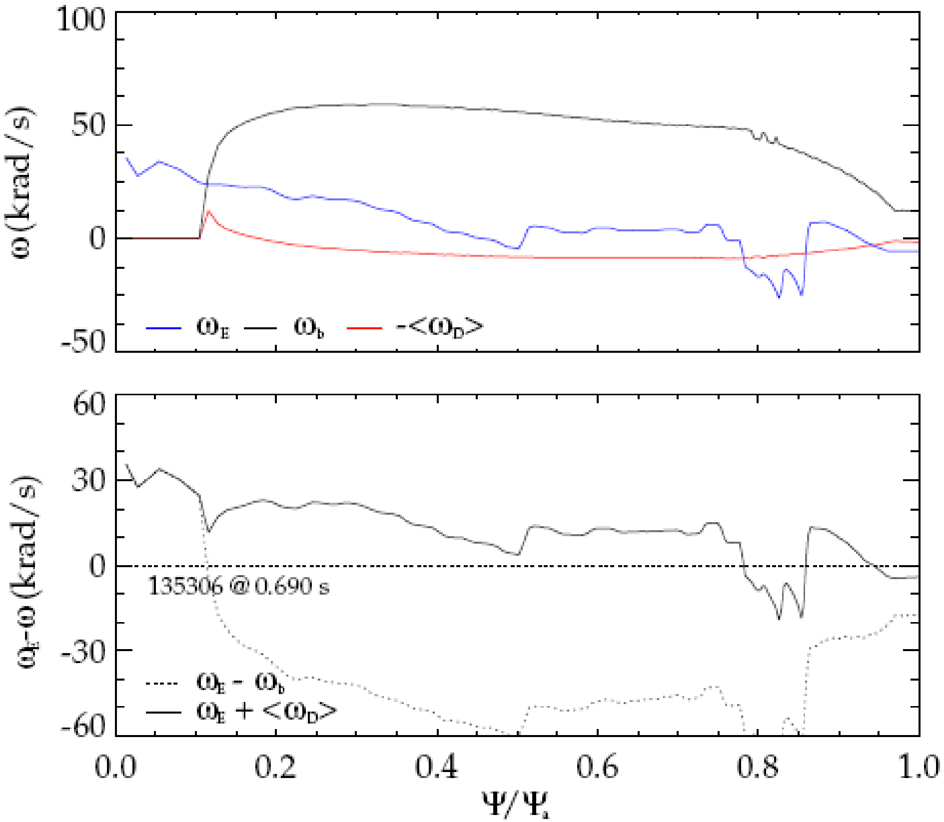

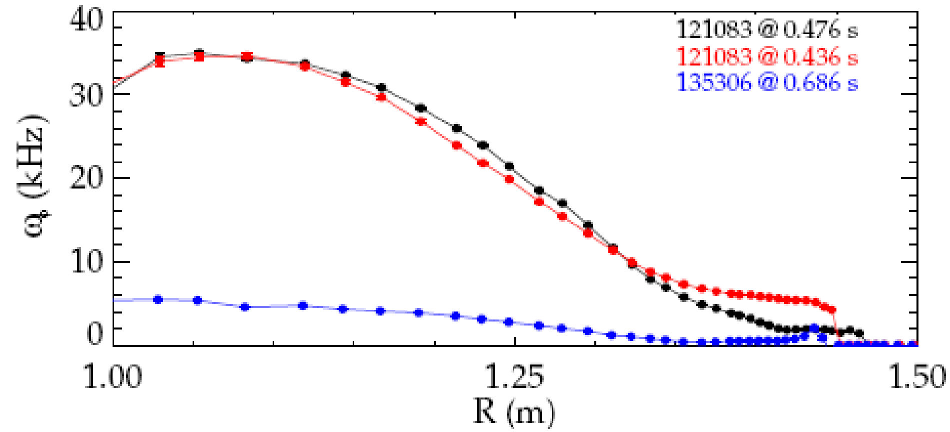

$$\delta W_K \sim \left[\frac{\omega_{*N} + \left(\hat{\varepsilon} - \frac{3}{2}\right)\omega_{*T} + \omega_E - \omega_r - i\gamma}{\langle \omega_D \rangle + l\omega_b - i\nu_{\text{eff}} + \omega_E - \omega_r - i\gamma} \right]$$

$$\omega_E = \omega_\phi - \omega_{*i}$$

- Stable cases in precession drift resonance at “low” rotation

Thermal ions are most important contributors to stability

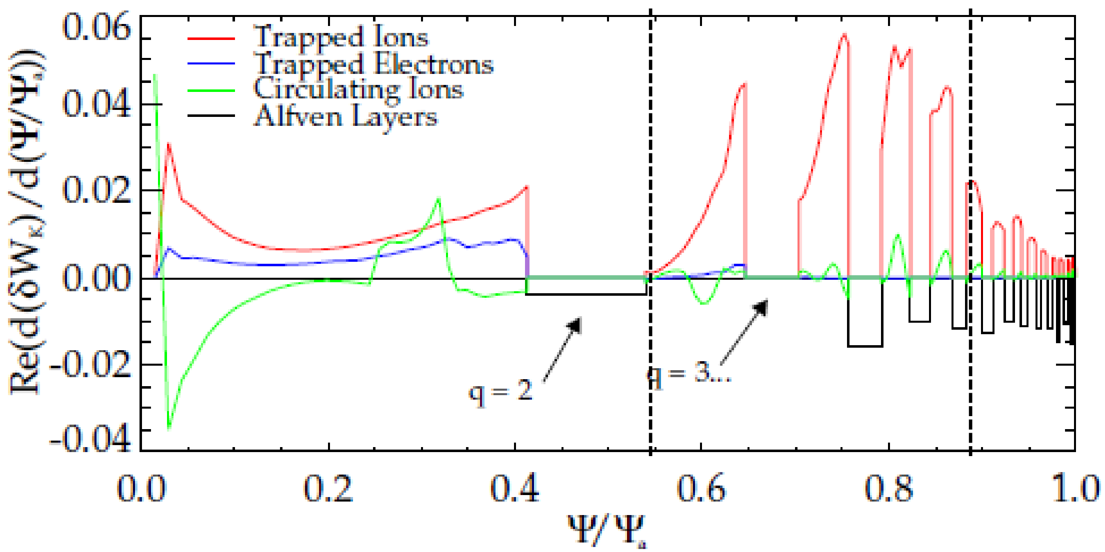

- Examine δW_K from each particle type vs. Ψ
  - Flat areas are rational surface layers (integer q ± 0.2).
  - Thermal ions are the most important contributor to stability.
- Entire profile is important, but q > 2 contributes ~60%
  - RWM eigenfunction is large in this region.
  - Temperature and density gradients are large (ω_{*N}, ω_{*T} large).

The dispersion relation can be rewritten in a form convenient for making stability diagrams

- Solve for γ in terms of Re(δW$_K$) and Im(δW$_K$).
  - Contours of constant γ form circles on a stability diagram of Im(δW$_K$) vs. Re(δW$_K$).

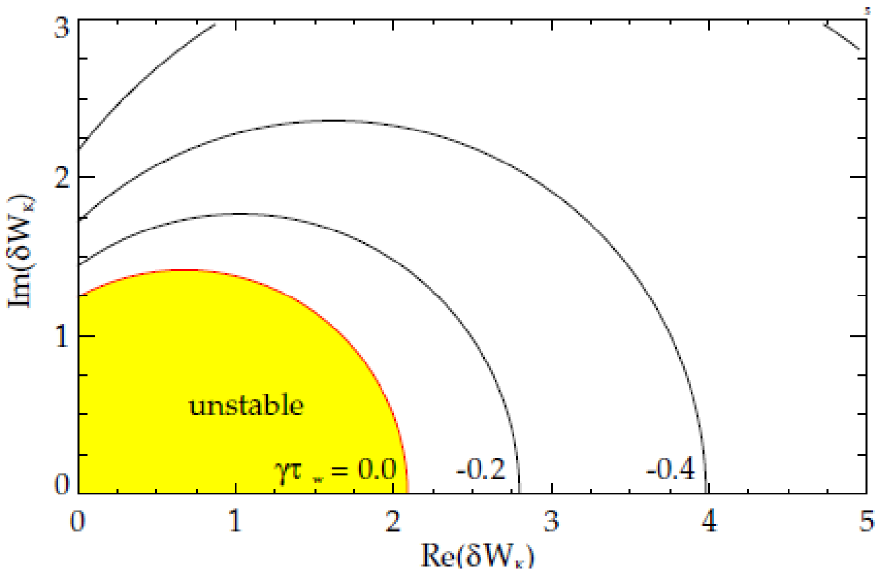

$$(\gamma - i\omega_r)\tau_w = -\frac{\delta W_\infty + \delta W_K}{\delta W_b + \delta W_K}$$

$$(Re\,(\delta W_K) - a)^2 + (Im\,(\delta W_K))^2 = r^2$$

$$r = \frac{1}{2}\,(\delta W_b - \delta W_\infty)\,\frac{1}{(1+\gamma\tau_w)}$$

$$\begin{aligned} a \;=\; & -\frac{1}{2}\,(\delta W_b + \delta W_\infty) \\ & -\frac{1}{2}\,(\delta W_b - \delta W_\infty)\,\frac{\gamma\tau_w}{1+\gamma\tau_w} \end{aligned}$$

Scaling the experimental rotation profile illuminates the complex relationship between rotation and stability

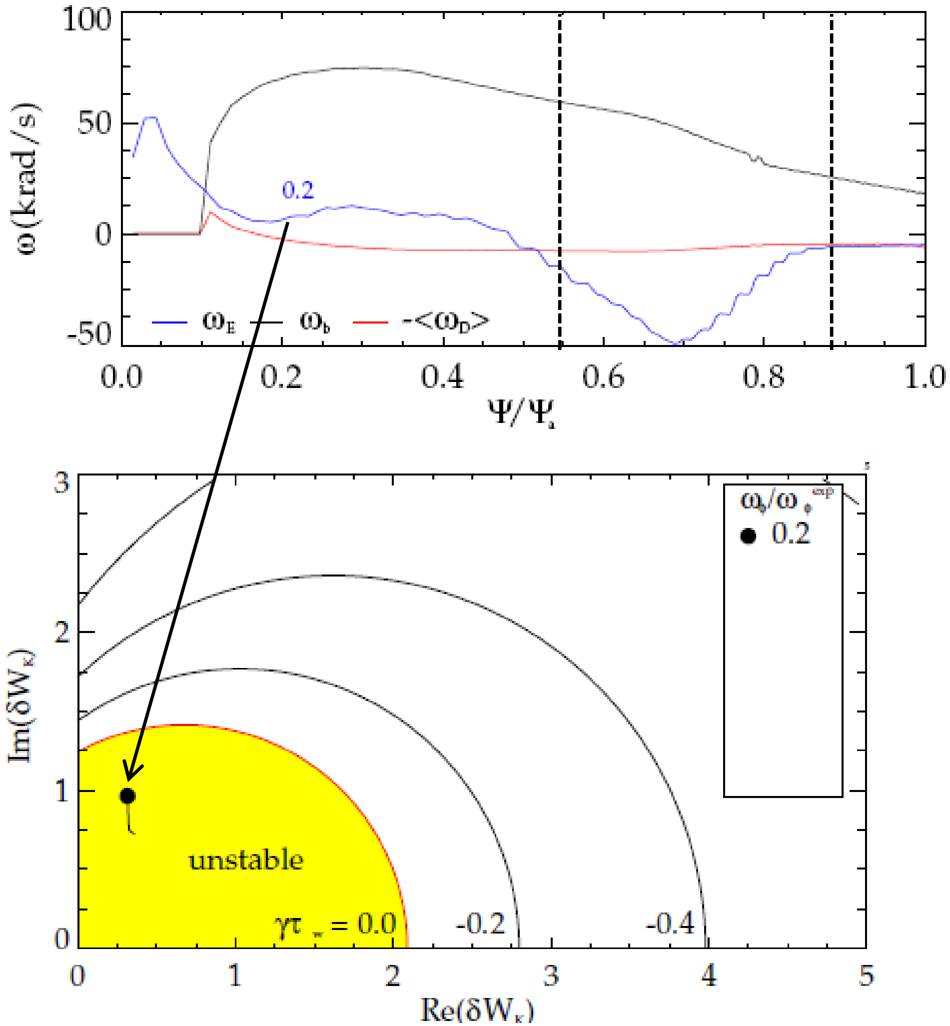

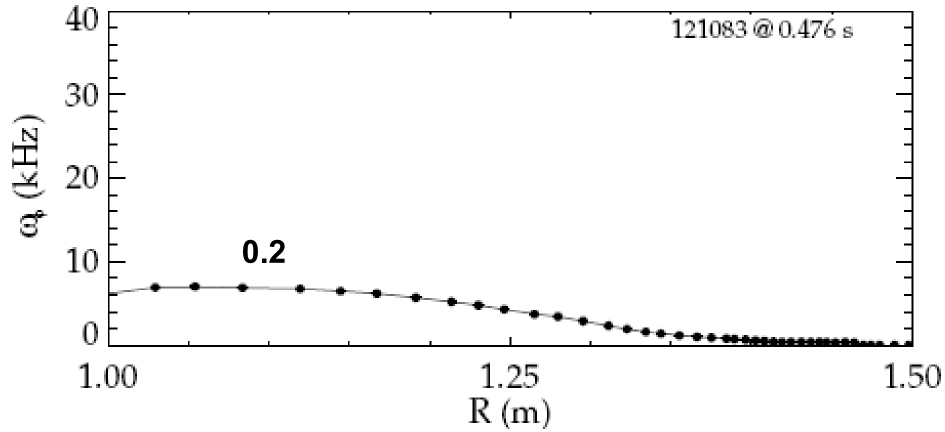

- Rotation profile scan:
  - 0.2: Instability at low rotation.

Scaling the experimental rotation profile illuminates the complex relationship between rotation and stability

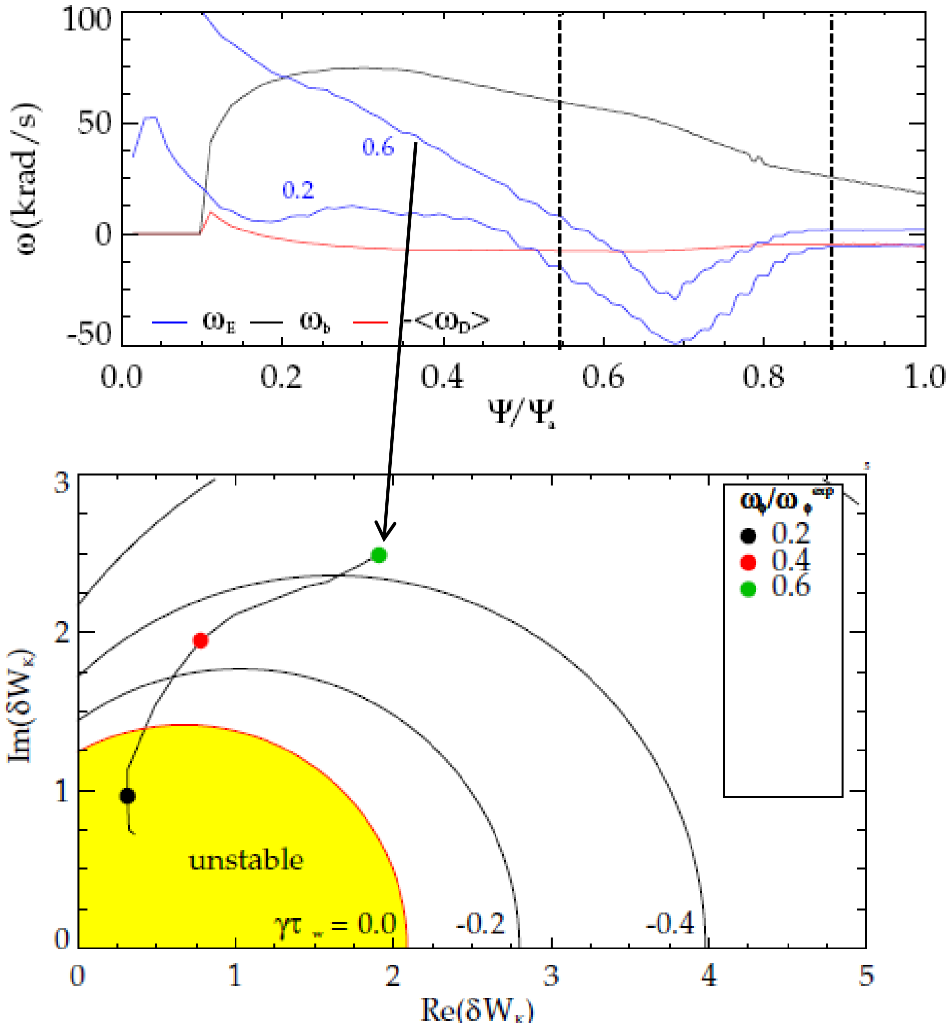

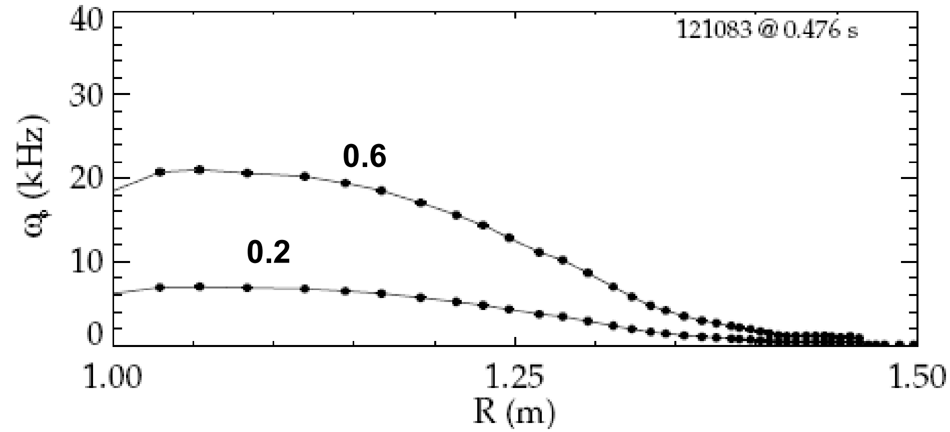

- Rotation profile scan:
  - 0.2: Instability at low rotation.
  - 0.6: Stable: ω_D resonance.

Scaling the experimental rotation profile illuminates the complex relationship between rotation and stability

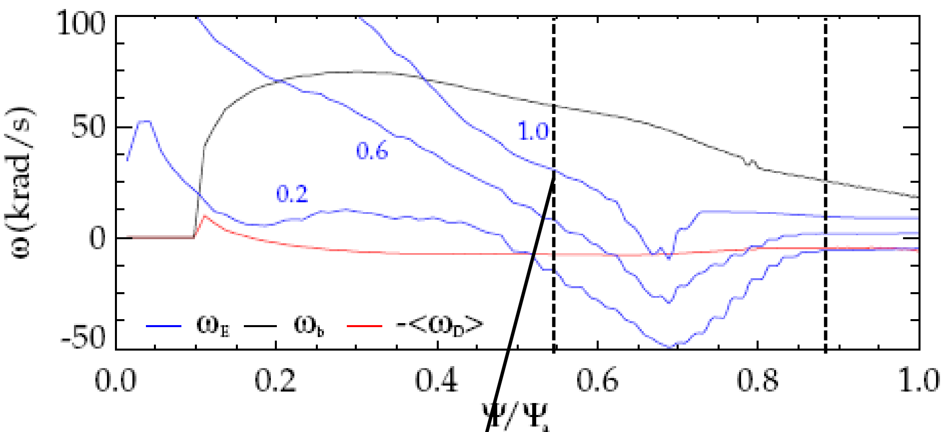

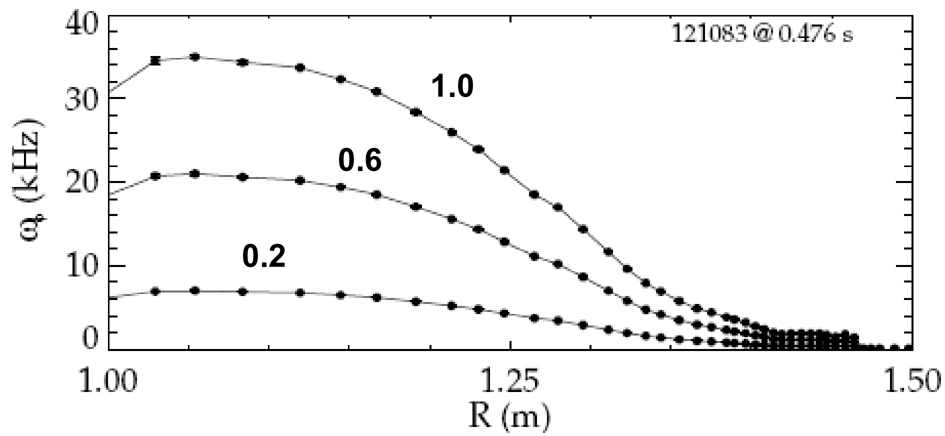

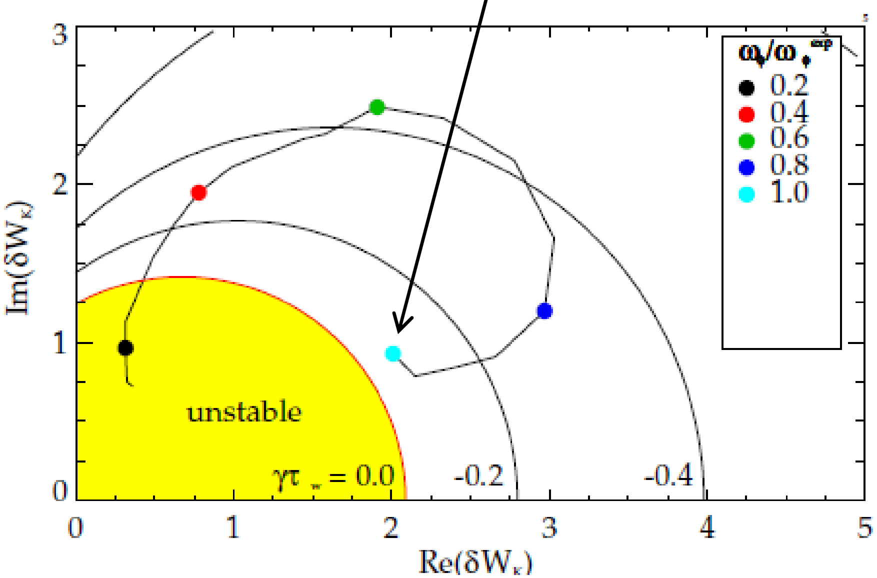

- Rotation profile scan:
  - 0.2: Instability at low rotation.
  - 0.6: Stable: ω_D resonance.
  - 1.0: Marginal: in-between resonances (actual experimental instability).

Scaling the experimental rotation profile illuminates the complex relationship between rotation and stability

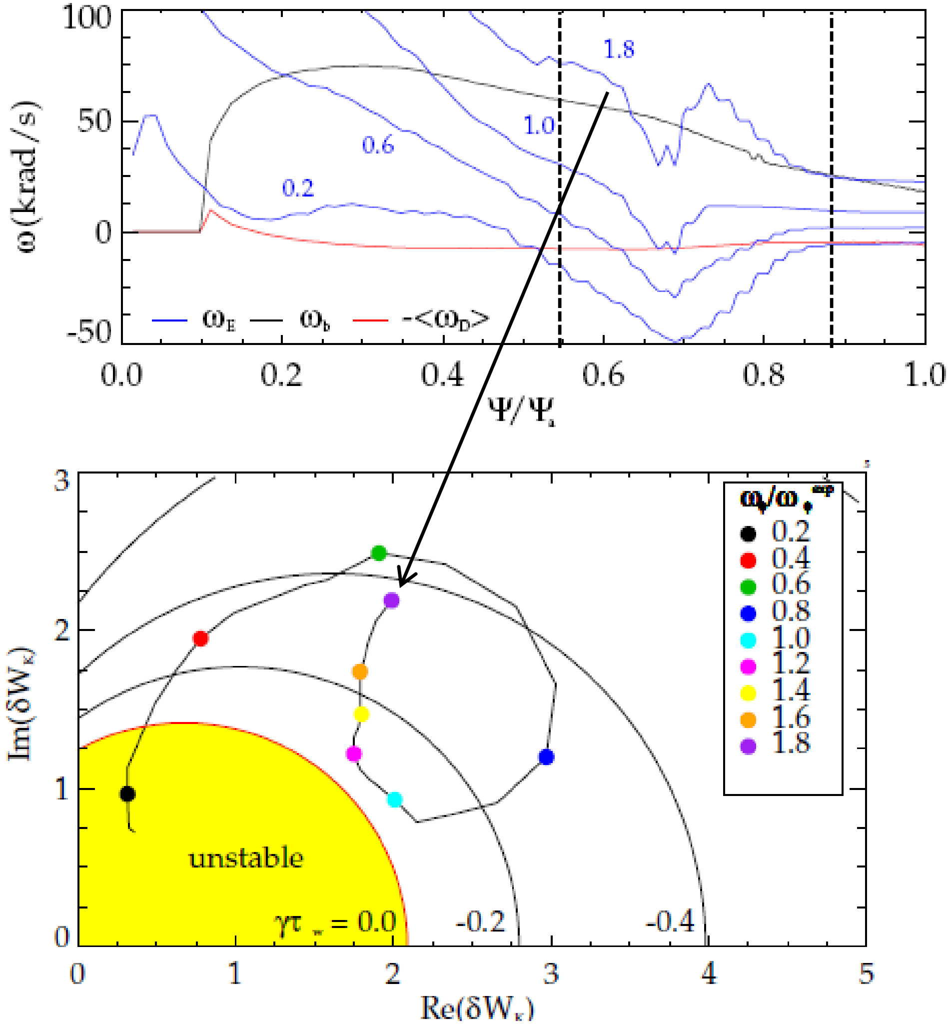

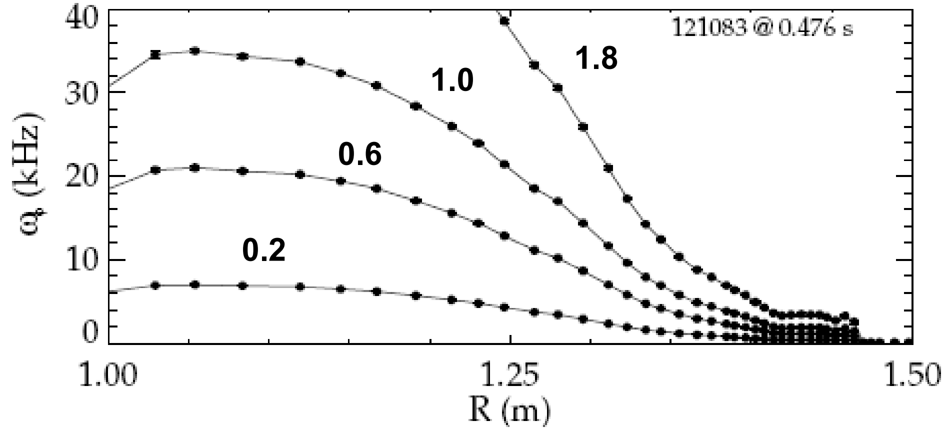

- Rotation profile scan:
  - 0.2: Instability at low rotation.
  - 0.6: Stable: ω_D resonance.
  - 1.0: Marginal: in-between resonances (actual experimental instability).
  - 1.8: Stable: ω_b resonance.

Scaling the experimental rotation profile illuminates the complex relationship between rotation and stability

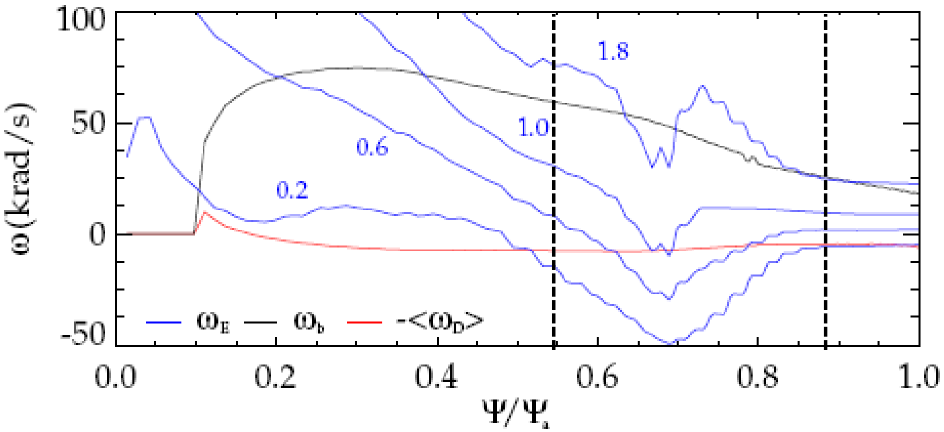

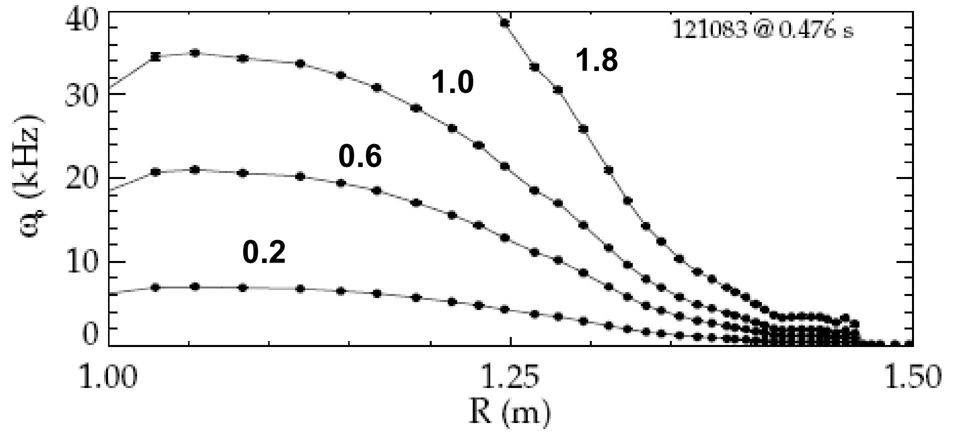

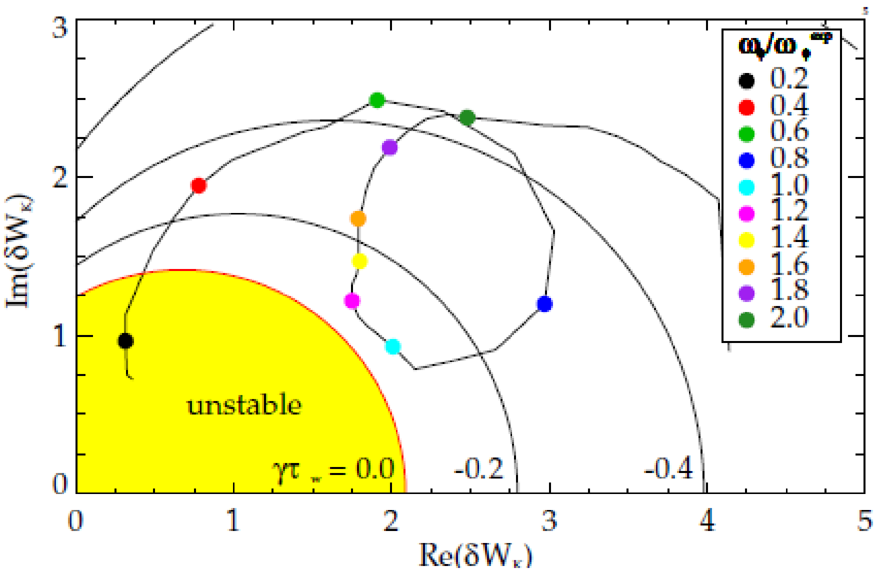

- Rotation profile scan:
  - 0.2: Instability at low rotation.
  - 0.6: Stable: ω_D resonance.
  - 1.0: Marginal: in-between resonances (actual experimental instability).
  - 1.8: Stable: ω_b resonance.

The weakened stability rotation gap is altered by changing collisionality

- Scan of ω_ϕ and collisionality
  - scale *n* & *T* at constant β
  - Changing *ν* shifts the rotation of weakened stability.

$$\delta W_K \sim \left[\frac{\omega_{*N} + \left(\hat{\varepsilon} - \frac{3}{2}\right)\omega_{*T} + \omega_E - \omega_r - i\gamma}{\langle \omega_D \rangle + l\omega_b - i\nu_{\text{eff}} + \omega_E - \omega_r - i\gamma} \right]$$

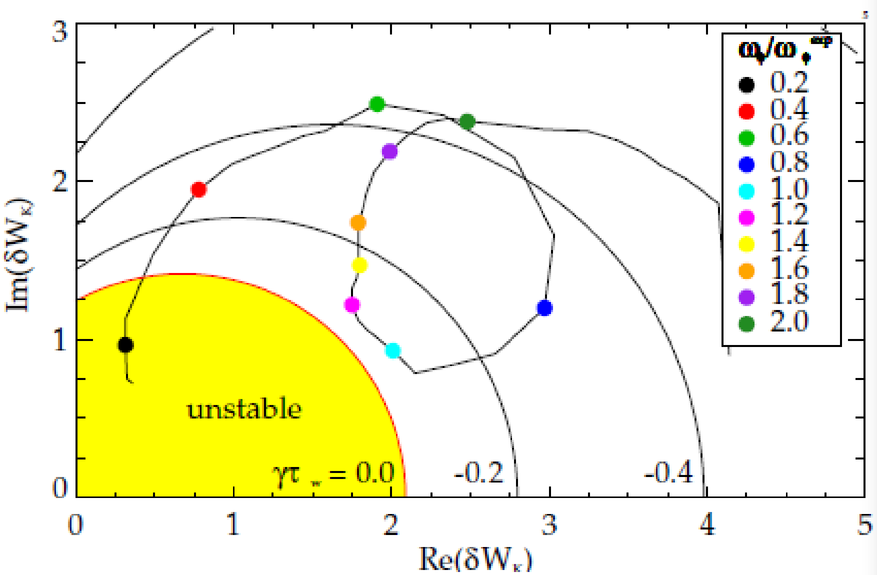

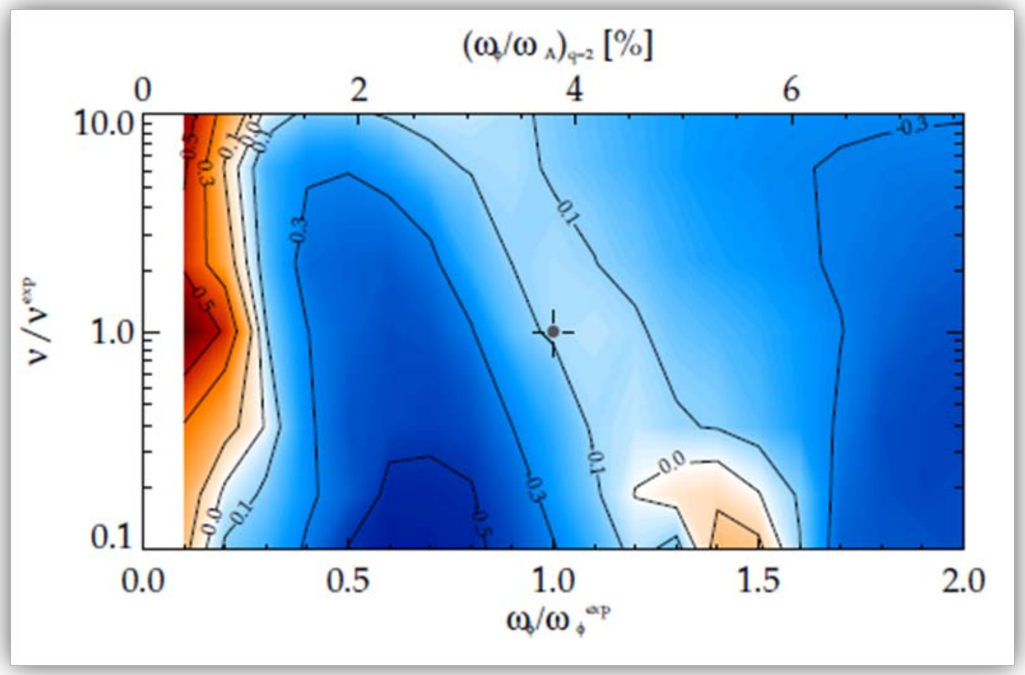

The weakened stability rotation gap is altered by changing collisionality

- Scan of ω_ϕ and collisionality
  - scale *n* & *T* at constant β
  - Changing *ν* shifts the rotation of weakened stability.

$$\delta W_K \sim \left[\frac{\omega_{*N} + \left(\hat{\varepsilon} - \frac{3}{2}\right)\omega_{*T} + \omega_E - \omega_r - i\gamma}{\langle\omega_D\rangle + l\omega_b - i\nu_{\mathrm{eff}} + \omega_E - \omega_r - i\gamma}\right]$$

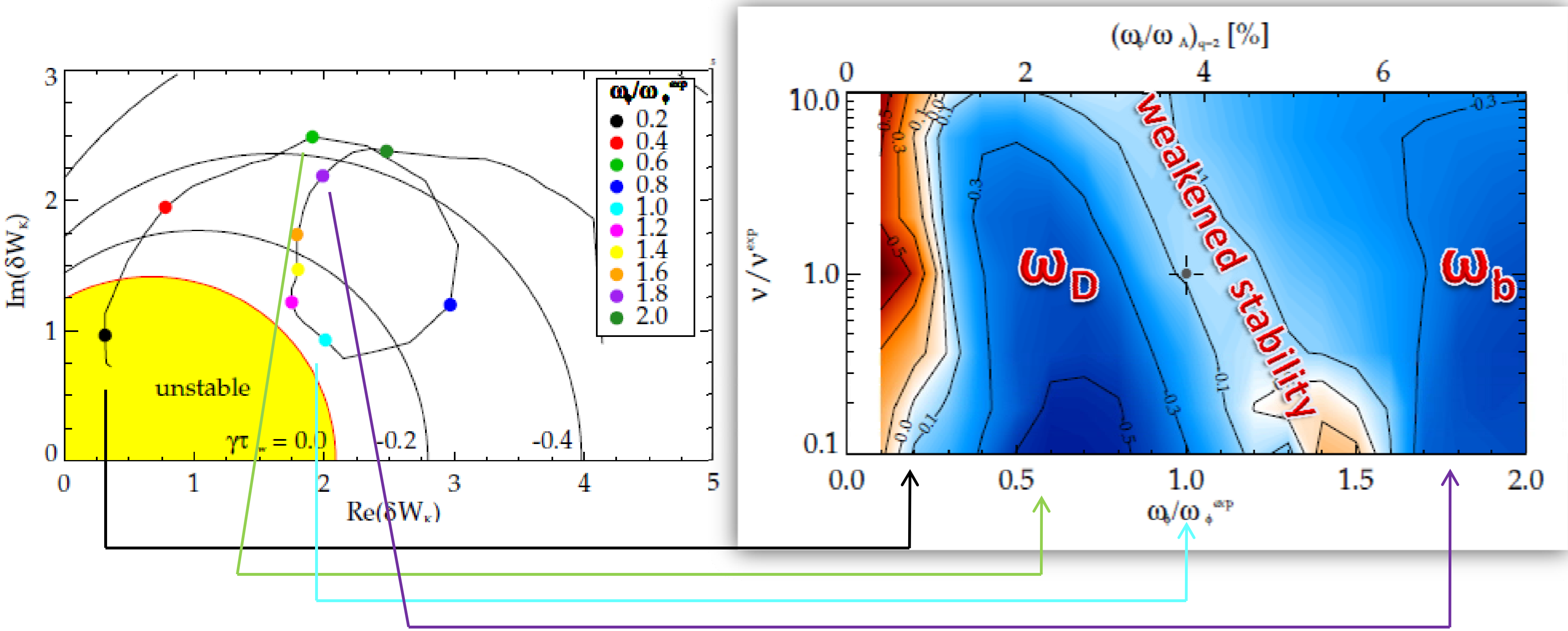

Widely different experimentally marginally stable rotation profiles each are in the gap between stabilizing resonances

- Each shot has a ω_ϕ with weakened stability.
  - Sometimes that stability reduction is not enough to quantitatively reach marginal.

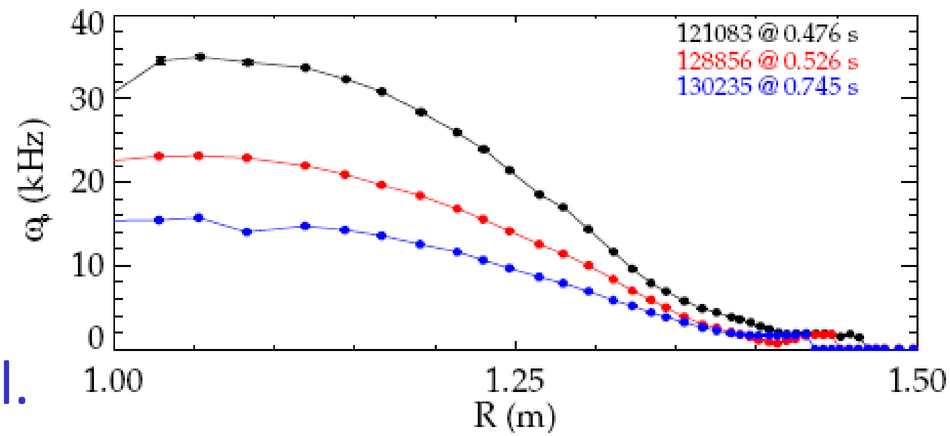

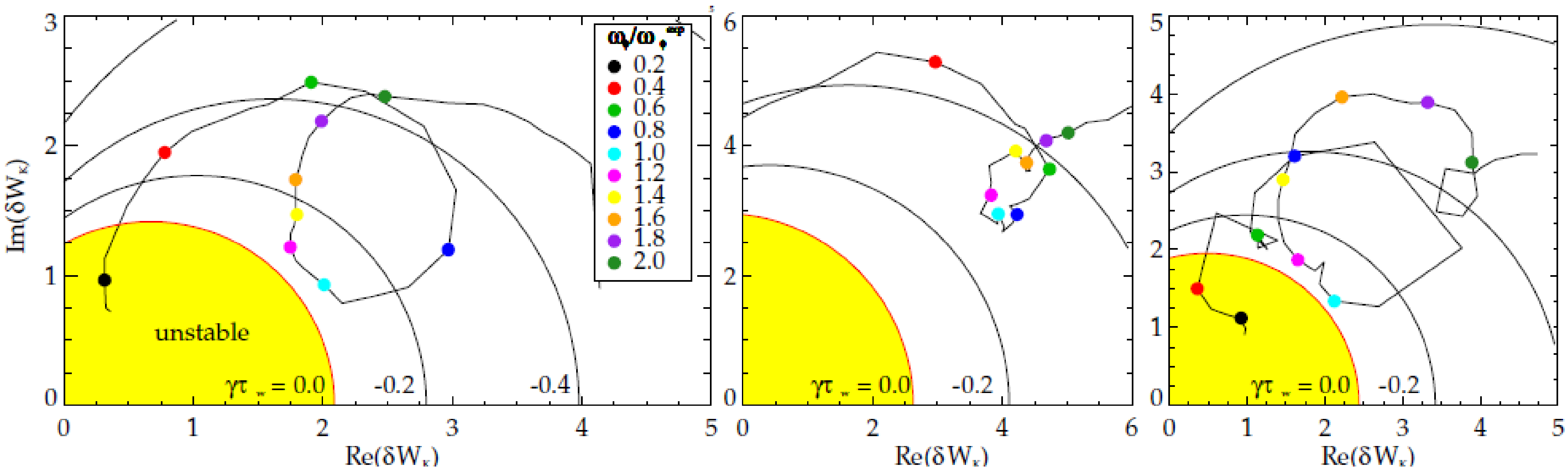

121083 @ 0.475 s

128856 @ 0.526 s

130235 @ 0.745 s

Improvements to the theory and calculation, to use as a quantitative predictor of instability

1. Examine sensitivity of calc.

- Non-linear inclusion of ω_r and γ: Iteration (τ_w = 1ms)
- Sensitivities to inputs: ex: Δq = 0.15 – 0.25

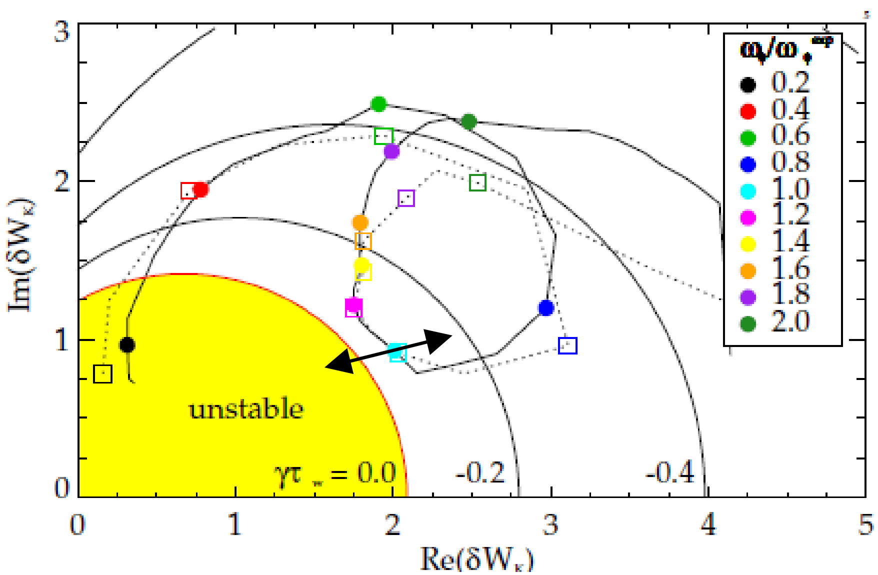

121083 @ 0.475 s

2. Include energetic particles

- Important stabilizing kinetic effects in theory
- E.P. modes known to "trigger" RWM in experiment

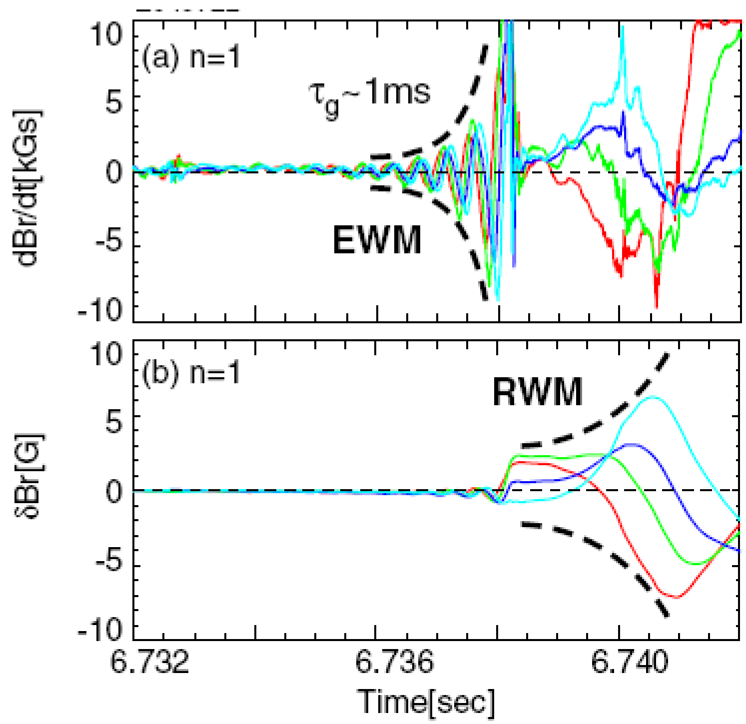

(Matsunaga et al., PRL, 2009)

Present inclusion of energetic particles in MISK: isotropic slowing down distribution (ex. alphas in ITER)

Thermal Particles: Maxwellian

$$\delta W_K \sim \left[\frac{\omega_{*N} + \left(\hat{\varepsilon} - \frac{3}{2}\right)\omega_{*T} + \omega_E - \omega_r - i\gamma}{\langle \omega_D \rangle + l\omega_b - i\nu_{\mathrm{eff}} + \omega_E - \omega_r - i\gamma} \right]$$

E.P.s: Slowing-down

$$f(\varepsilon, \Psi) = \frac{C(\Psi)}{\varepsilon^{\frac{3}{2}} + \varepsilon_c^{\frac{3}{2}}}$$

- E.P. resonances add to δW_K, lead to greater stability
  - May be overestimating thermal part, E.P. part may lead to marginal
- Example: α particles in ITER
  - Higher β_α leads to greater stability
  - Isotropic f is a good approx.

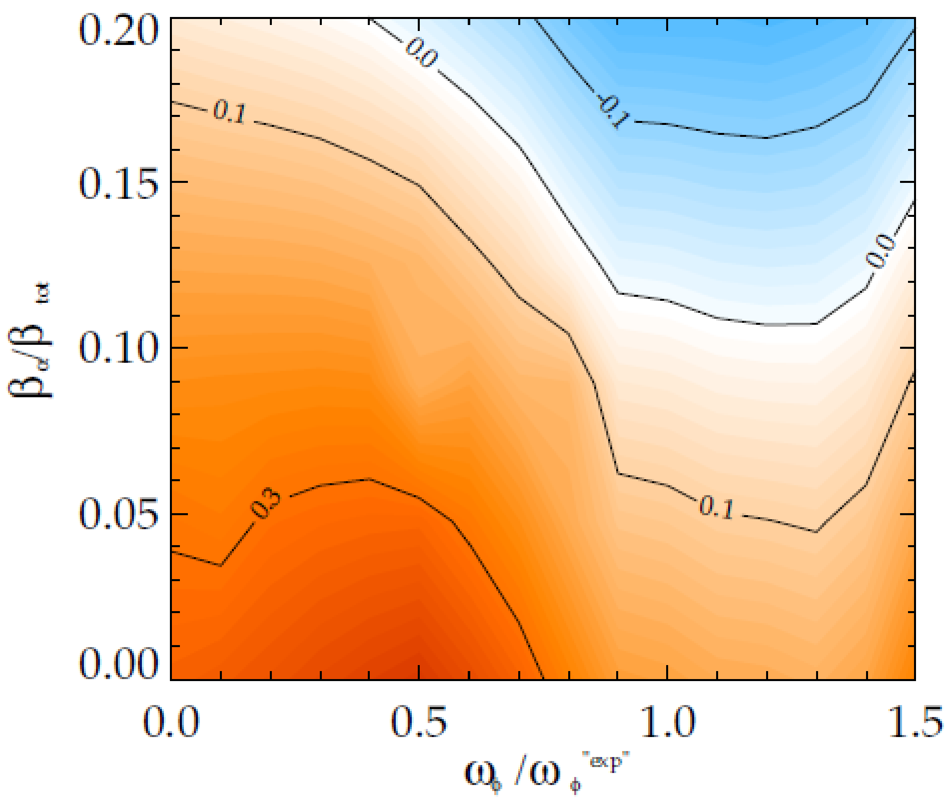

NSTX and DIII-D experiments in 2009 explored the effect of energetic particles on RWM stability

DIII-D Experiment (with Reimerdes)

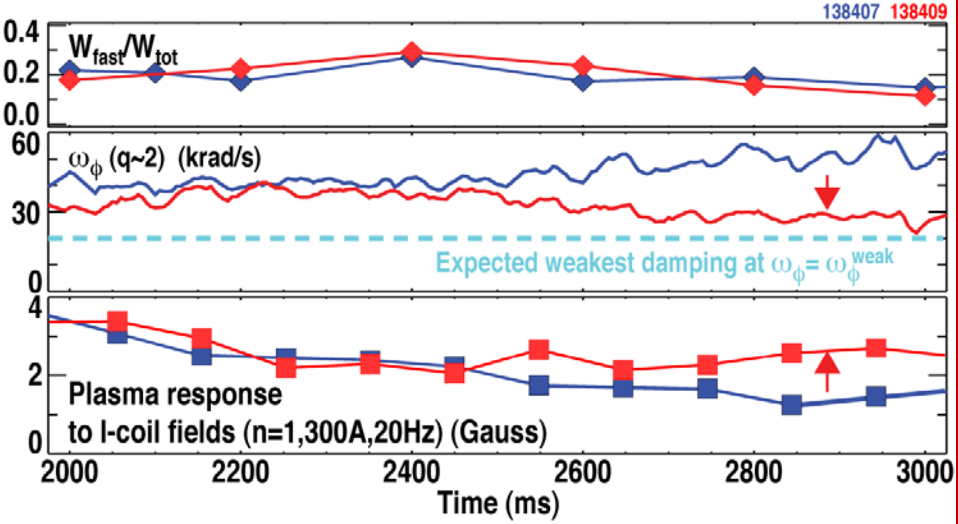

- Higher n_e and I_p reduced W_f/W_t by 40% over previous exp.
- RWM remains stable, but response higher as $\omega_\phi \rightarrow \omega_\phi^{weak}$

NSTX Experiment

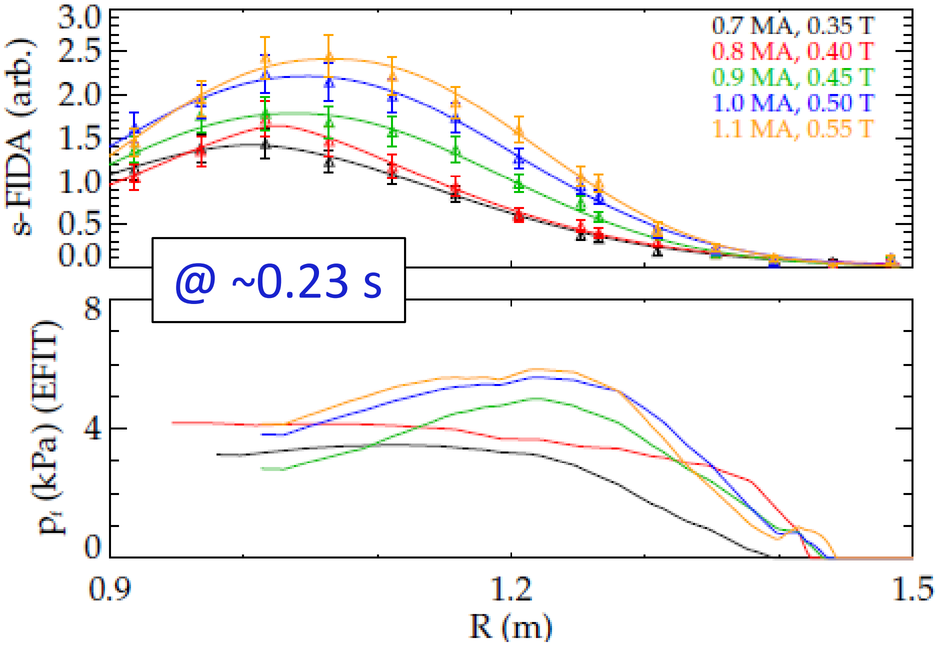

- FIDA, EFIT, and TRANSP confirm p_f scan with B_t, I_p
- RWM unstable cases found for each p_f.

Energetic particles contribute linearly to RWM stability in NSTX

- Adding energetic particles adds a significant $\Delta\gamma$
  - independent of ω_ϕ, since $\omega_D(\varepsilon)$ and $\omega_b(\varepsilon^{½}) >> \omega_E$, meaning energetic particles are <u>not</u> in mode resonance
- Despite this, these shots experimentally went unstable
  - Weakened thermal particle stabilization at marginal ω_ϕ is enough to destabilize the mode

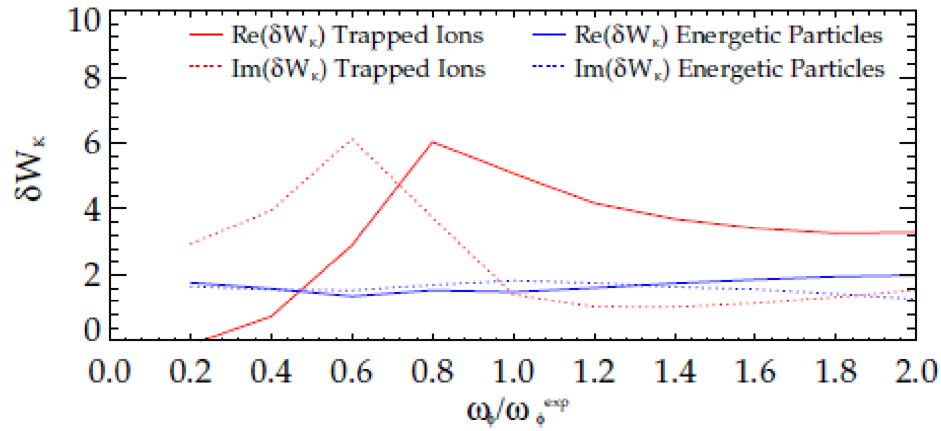

NSTX 121090 @ 0.6 s

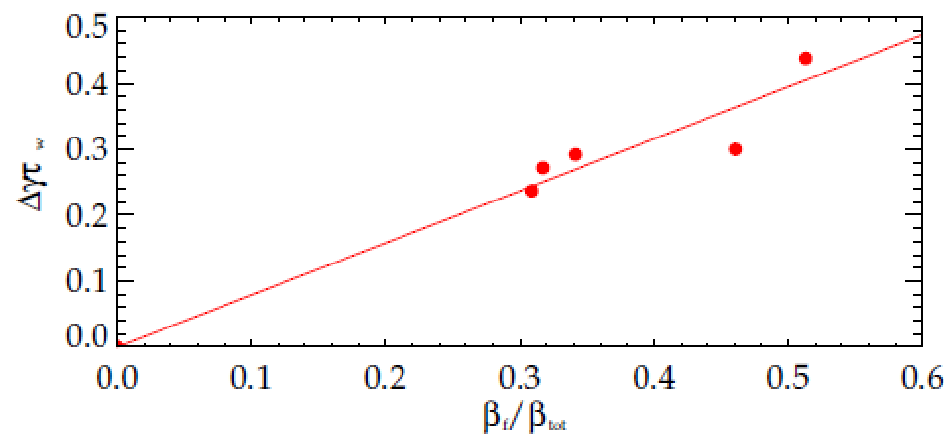

Various NSTX discharges at marginal stability (Note: ignores profile effects)

In NSTX…

- XXX
  - XXX
- XXX
  - XXX

A new, more accurate energetic particle distribution function is being implemented

- Presently *f* is considered independent of χ.
  - Not a good approximation for beam ions
  - Overpredicts trapped frac.:

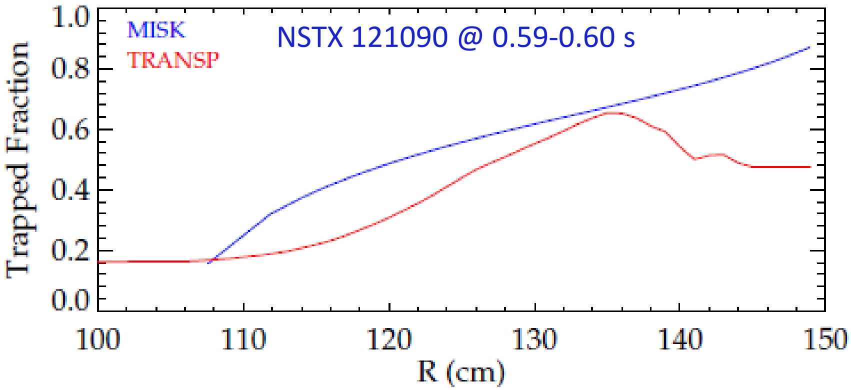

- Future:
  - Use *f* from TRANSP directly
  - Consider circulating E.P.s as well

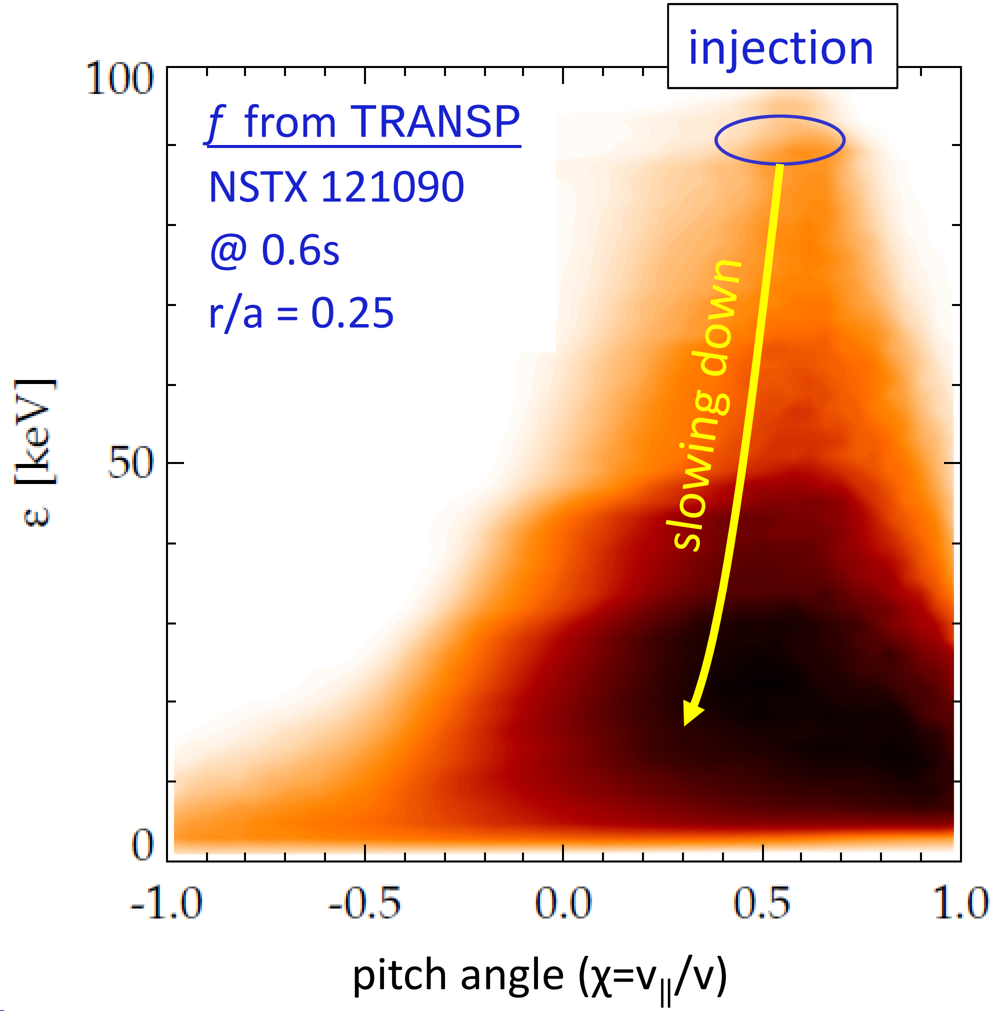

Kinetic RWM stability theory has a more complex relationship with ω_ϕ than simple theories.

- High plasma rotation alone is inadequate to ensure RWM stability in future devices
  - A weakened stability gap exists between ω_b and ω_D resonances.
  - Can use ω_ϕ control to stay away from gap and/or RWM active control to navigate through gap.
- Favorable comparison between NSTX exp. results and theory
  - Multiple NSTX discharges with widely different marginally stable ω_ϕ profiles fall in this gap.
- Energetic particles provide an important stabilizing effect

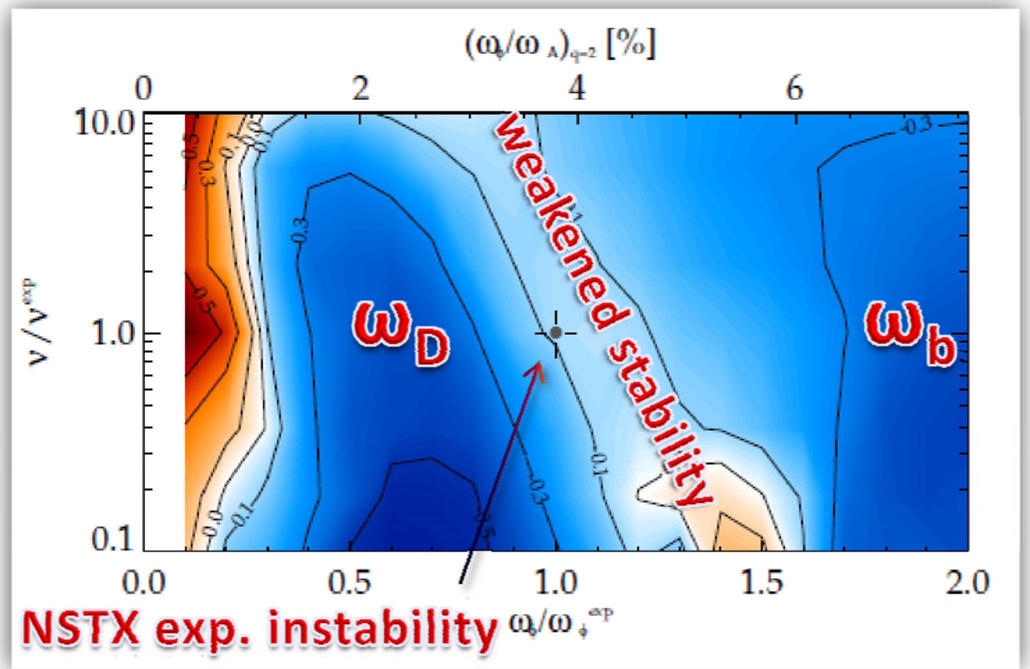

Visit the poster this afternoon for more detail

NSTX and DIII-D joint experiment in 2009 explored the effect of energetic particles on RWM stability

DIII-D Experiment (with Reimerdes)

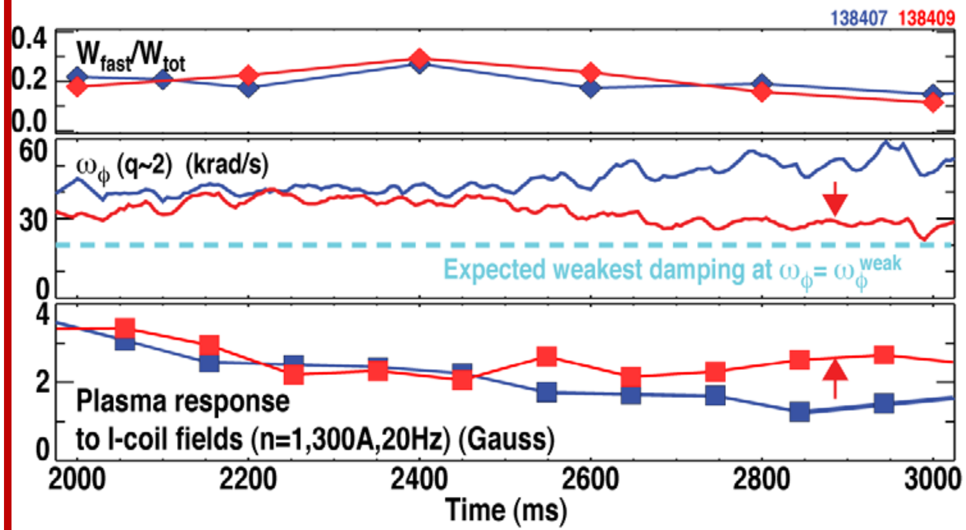

– Higher n_e and I_p reduced W_f/W_t by 40% over previous exp.

– RWM remains stable, but response higher as $\omega_\phi \rightarrow \omega_\phi^{weak}$

NSTX and DIII-D experiments in 2009 explored the effect of energetic particles on RWM stability

DIII-D Experiment (with Reimerdes)

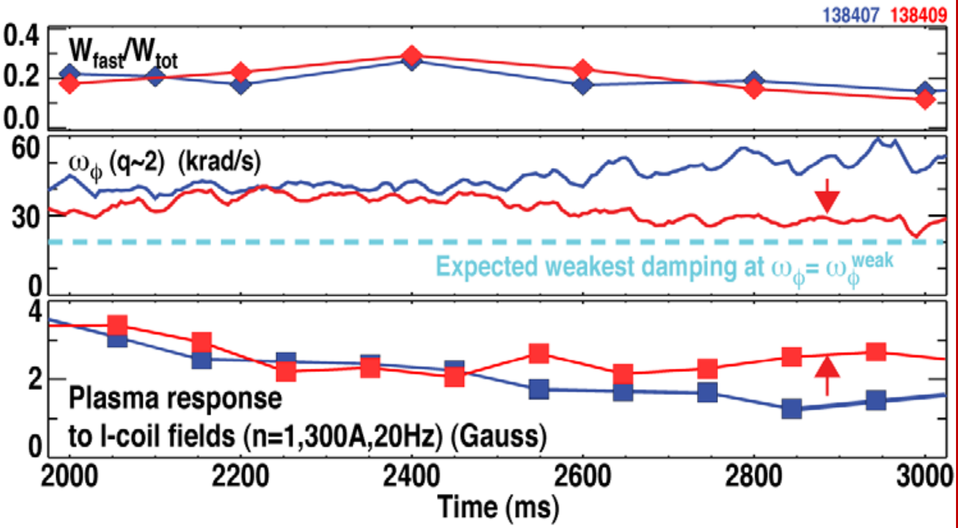

– Higher n_e and I_p reduced W_f/W_t by 40% over previous exp.

– RWM remains stable, but response higher as $\omega_\phi \rightarrow \omega_\phi^{weak}$

NSTX Experiment

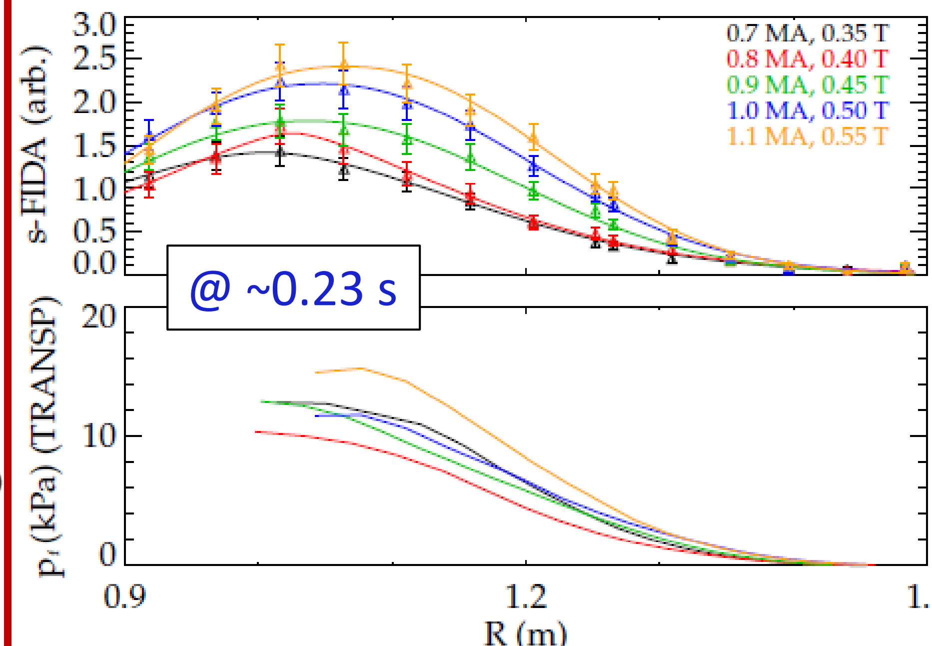

– FIDA, EFIT, and TRANSP confirm p_f scan with B_t, I_p

– RWM unstable cases found for each p_f.

NSTX and DIII-D experiments in 2009 explored the effect of energetic particles on RWM stability

DIII-D Experiment (with Reimerdes)

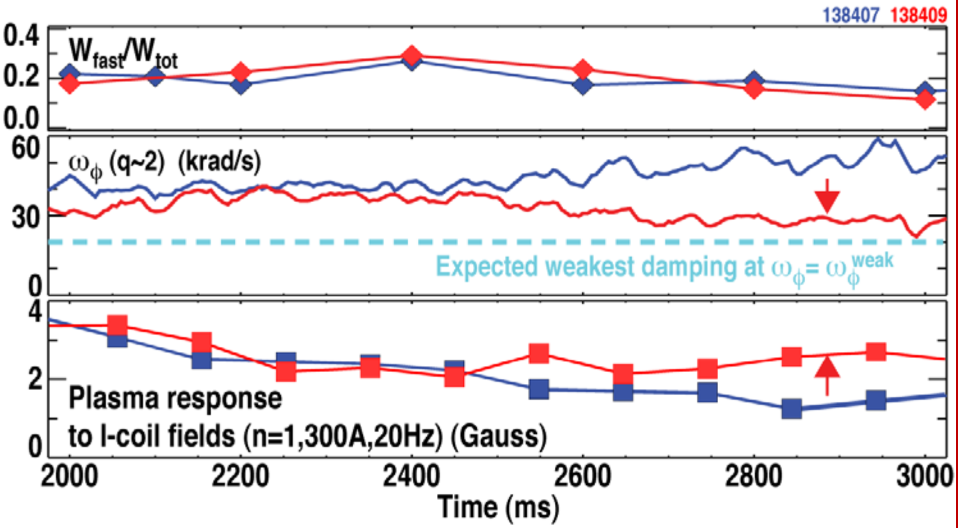

- Higher n_e and I_p reduced W_f/W_t by 40% over previous exp.
- RWM remains stable, but response higher as $\omega_\phi \rightarrow \omega_\phi^{weak}$

NSTX Experiment

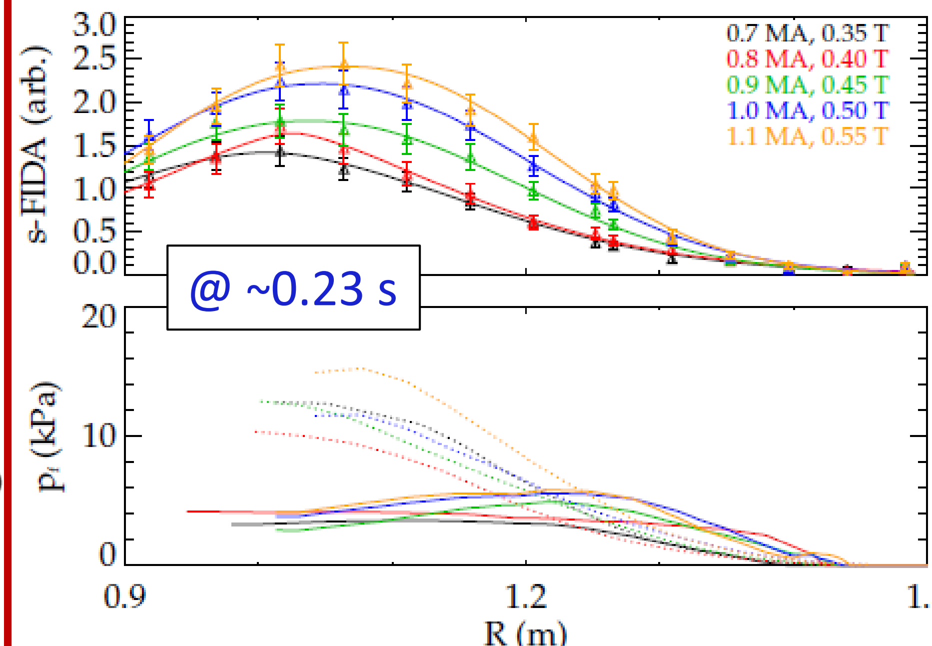

- FIDA, EFIT, and TRANSP confirm p_f scan with B_t, I_p
- RWM unstable cases found for each p_f.

A new, more accurate energetic particle distribution function is being implemented

- Presently *f* is considered independent of χ.
  - Not a good approximation for beam ions
  - Overpredicts trapped frac.:

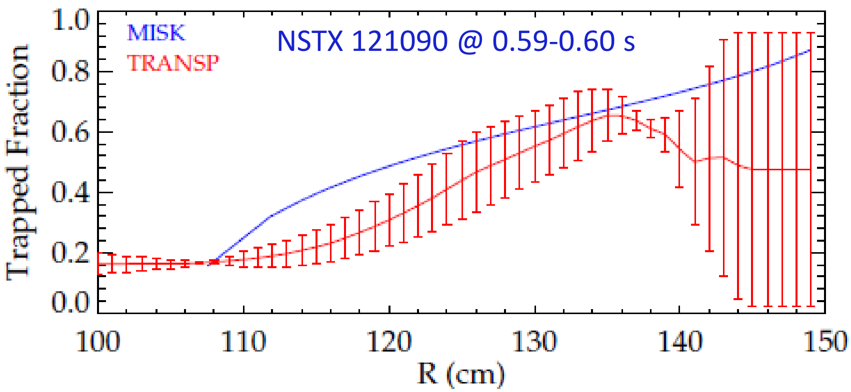

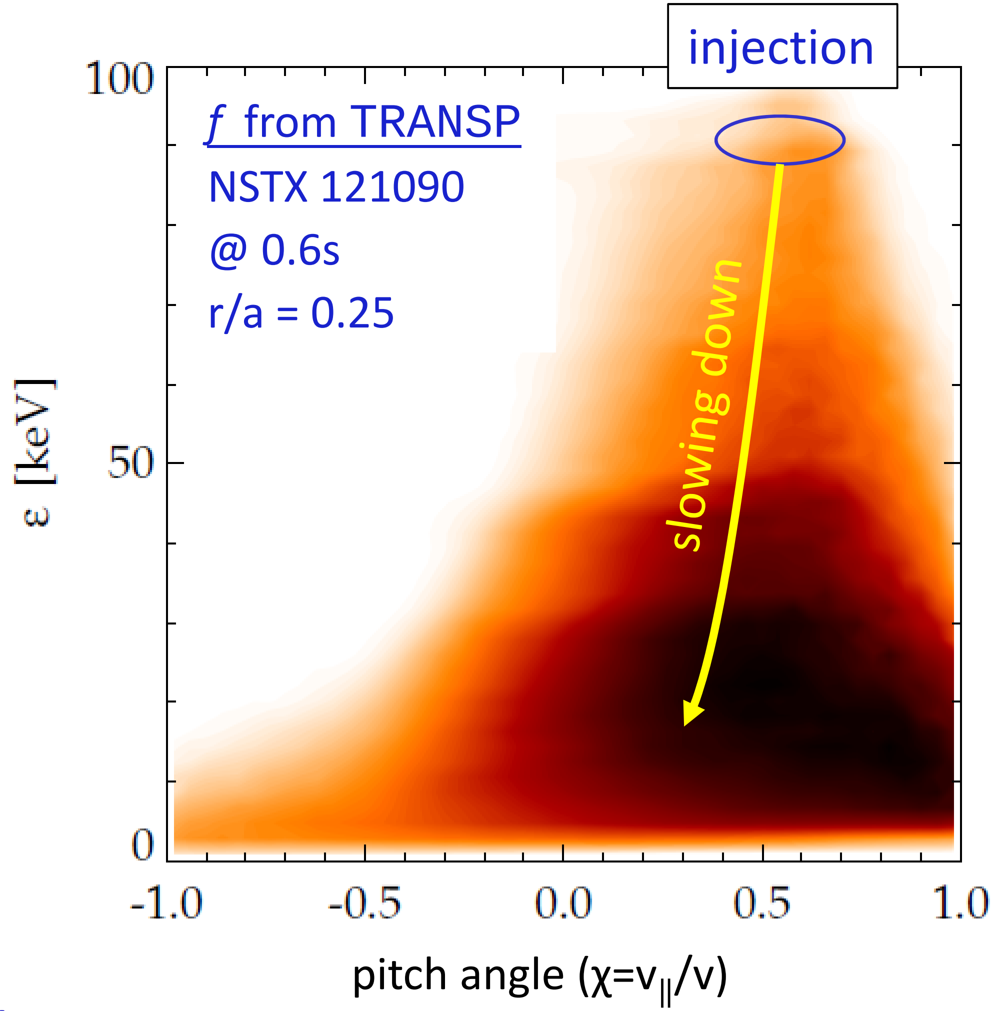

- Future:
  - Use *f* from TRANSP directly
  - Consider circulating E.P.s as well

Abstract

The Role of Kinetic Effects, Including Fast Particles, in Resistive Wall Mode Stability*

J.W. BERKERY, Columbia University**

Theoretically, the RWM is thought to be stabilized by energy dissipation mechanisms that depend on plasma rotation and other parameters, with kinetic effects being emphasized[1]. Experiments in NSTX show that the RWM can be destabilized in high rotation plasmas while low rotation plasmas can be stable, which calls into question the concept of a "critical" plasma rotation for stability. Also, recent results from JT-60U show that fast particle modes can trigger RWMs[2], indicating the importance of including kinetic fast particle resonances in the theory of RWM passive stabilization. The present work tests theoretical stabilization mechanisms against experimental discharges with various plasma rotation profiles created by applying either n=2 or 3 field configurations, and with various fast particle fractions. Kinetic modification of the ideal stability criterion is calculated with the MISK code, using experimental equilibrium reconstructions. Analysis of multiple NSTX discharges from just before RWM instability is observed, predicts near-marginal mode growth rates, with trapped ions providing the dominant kinetic resonances. Resonances with fast particles also provide an important stabilizing effect. Increasing or decreasing the rotation in the calculation drives the prediction farther from the marginal point in either the stable or unstable direction, showing that unlike simpler "critical" rotation theories, kinetic theory allows for a more complex relationship between plasma rotation and RWM stability. Kinetic theory also has the potential to explain how fast particle loss can trigger RWMs, through the loss of an important stabilization mechanism.

*Supported by U.S. DOE Contracts DE-FG02-99ER54524 and DE-AC02-76CH03073.
**In collaboration with S.A. Sabbagh, H. Reimerdes, R. Betti, and B. Hu.

[1] B. Hu, R. Betti, and J. Manickam, *Phys. Plasmas* **12** (2005) 057301.
[2] G. Matsunaga et al., IAEA 2008.

NSTX 121083 @ 0.475 RWM characteristics

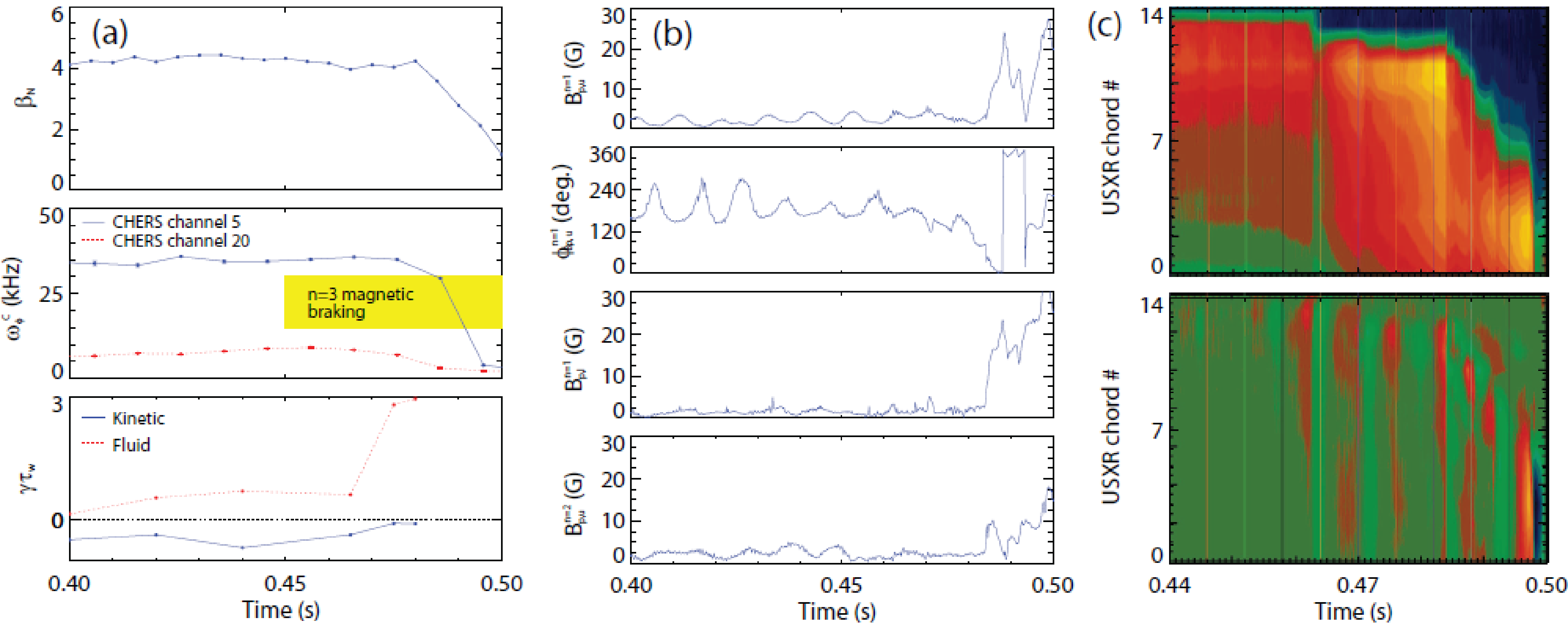

Present isotropic distribution function for energetic particles overestimates the trapped ion fraction

- First-order check:
  - MISK isotropic f overestimates the trapped ion fraction (compared to TRANSP).

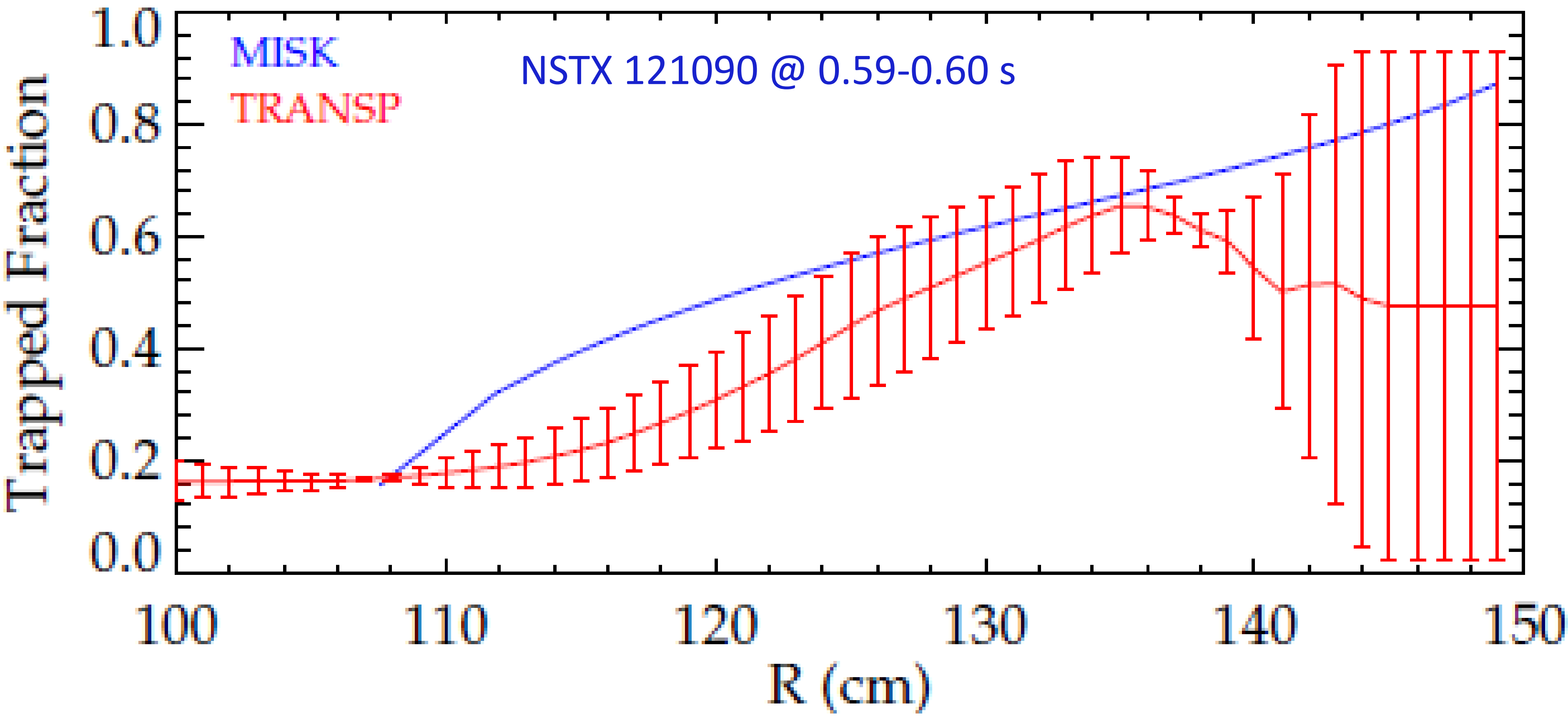

MISK sometimes overpredicts stability

unstable

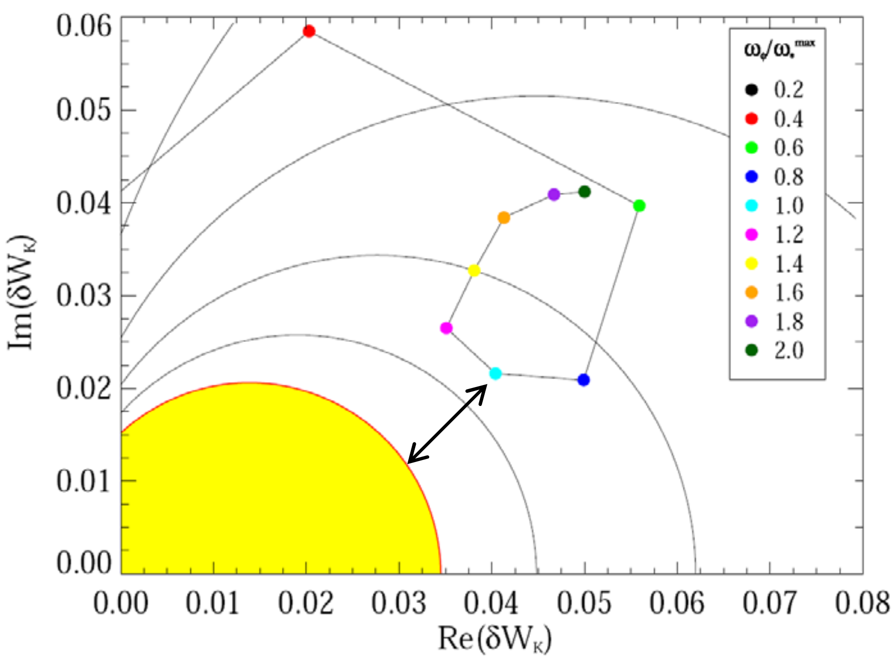

128856 @ 0.529

stable

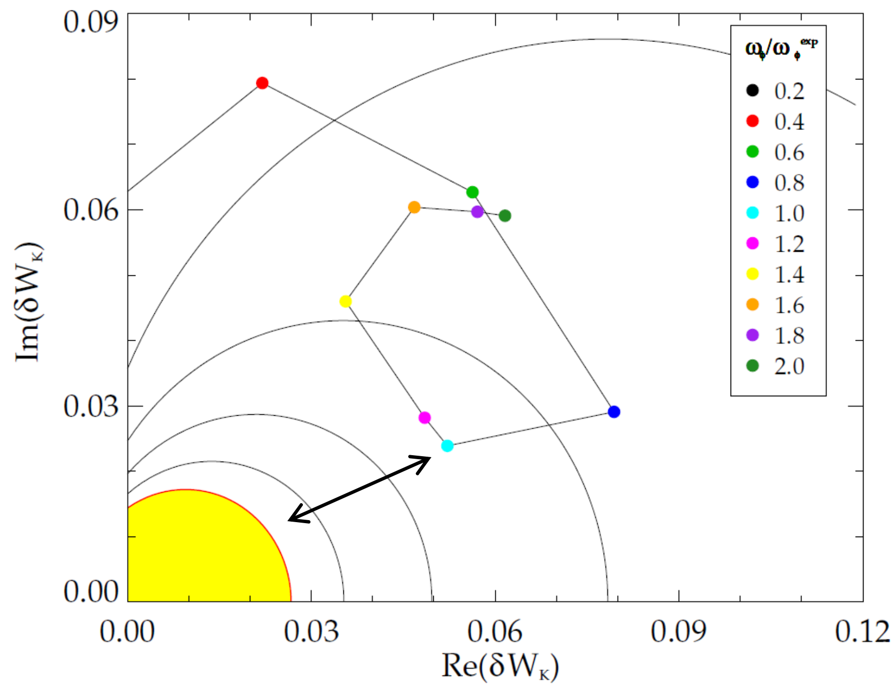

133367 @ 0.635

Perturbative vs. Self-consistent Approaches and Three Roots of the RWM Dispersion Relation

γ is found with a self-consistent or perturbative approach

The self-consistent (MARS) approach: solve for γ and ω from:

$$
\begin{aligned}
(\gamma + i(\omega_\phi - \omega))\tilde{\xi} &= \tilde{\mathbf{u}} - \mathbf{u}_0 \cdot \nabla \tilde{\xi} \\
\rho(\gamma + i(\omega_\phi - \omega))\tilde{\mathbf{u}} &= \mathbf{j} \times \tilde{\mathbf{B}} + \tilde{\mathbf{j}} \times \mathbf{B} - \nabla \cdot \tilde{\mathbf{P}} - \rho\left(\mathbf{u}_0 \cdot \nabla \tilde{\mathbf{u}} + \tilde{\mathbf{u}} \cdot \nabla \mathbf{u}_0\right) \\
\tilde{\mathbf{j}} &= \frac{1}{\mu_0} \boldsymbol{\nabla} \times \tilde{\mathbf{B}} \\
(\gamma + i(\omega_\phi - \omega))\tilde{\mathbf{B}} &= \nabla \times (\mathbf{u} \times \mathbf{B}) - \mathbf{u}_0 \cdot \nabla \tilde{\mathbf{B}} \\
(\gamma + i(\omega_\phi - \omega))\tilde{\mathbf{P}} &= -\tilde{\mathbf{u}} \cdot \boldsymbol{\nabla} \mathbf{P} \\
\boldsymbol{\nabla} \cdot \tilde{\mathbf{P}} &= \boldsymbol{\nabla} \tilde{p} + \nabla \cdot \left[\tilde{p}_\perp^K \mathbf{I} + (\tilde{p}_\parallel^K - \tilde{p}_\perp^K)\hat{\mathbf{b}}\hat{\mathbf{b}}\right].
\end{aligned}
$$

The perturbative (MISK) approach: solve for γ and ω from:

$$
(\gamma - i\omega)\tau_w = -\frac{\delta W_\infty + \delta W_K}{\delta W_b + \delta W_K}
$$

with δW_∞ and δW_b from PEST. There are three main differences between the approaches:

1. The way that rational surfaces are treated.
2. Whether ξ is changed or unchanged by kinetic effects.
3. Whether γ and ω are non-linearly included in the calculation.

Rational surfaces are treated differently

The self-consistent (MARS) approach: solve for γ and ω from:

$$
\begin{aligned}
(\gamma + i(\omega_\phi - \omega))\tilde{\xi} &= \tilde{\mathbf{u}} - \mathbf{u}_0 \cdot \nabla \tilde{\xi} \\
\rho(\gamma + i(\omega_\phi - \omega))\tilde{\mathbf{u}} &= \mathbf{j} \times \tilde{\mathbf{B}} + \tilde{\mathbf{j}} \times \mathbf{B} - \nabla \cdot \tilde{\mathbf{P}} - \rho\left(\mathbf{u}_0 \cdot \nabla \tilde{\mathbf{u}} + \tilde{\mathbf{u}} \cdot \nabla \mathbf{u}_0\right) \\
\tilde{\mathbf{j}} &= \frac{1}{\mu_0} \boldsymbol{\nabla} \times \tilde{\mathbf{B}} \\
(\gamma + i(\omega_\phi - \omega))\tilde{\mathbf{B}} &= \nabla \times (\mathbf{u} \times \mathbf{B}) - \mathbf{u}_0 \cdot \nabla \tilde{\mathbf{B}} \\
(\gamma + i(\omega_\phi - \omega))\tilde{\mathbf{P}} &= -\tilde{\mathbf{u}} \cdot \boldsymbol{\nabla} \mathbf{P} \\
\boldsymbol{\nabla} \cdot \tilde{\mathbf{P}} &= \boldsymbol{\nabla} \tilde{p} + \nabla \cdot \left[\tilde{p}_\perp^K \mathbf{I} + (\tilde{p}_\parallel^K - \tilde{p}_\perp^K)\hat{\mathbf{b}}\hat{\mathbf{b}}\right].
\end{aligned}
$$

MARS-K: "continuum damping included through MHD terms". This term includes parallel sound wave damping.

In MISK a layer of surfaces at a rational ±Δq is removed from the calculation and treated separately through shear Alfvén damping.

Unchanging ξ may be a good assumption

For DIII-D shot 125701, the eignfunction doesn't change due to kinetic effects.

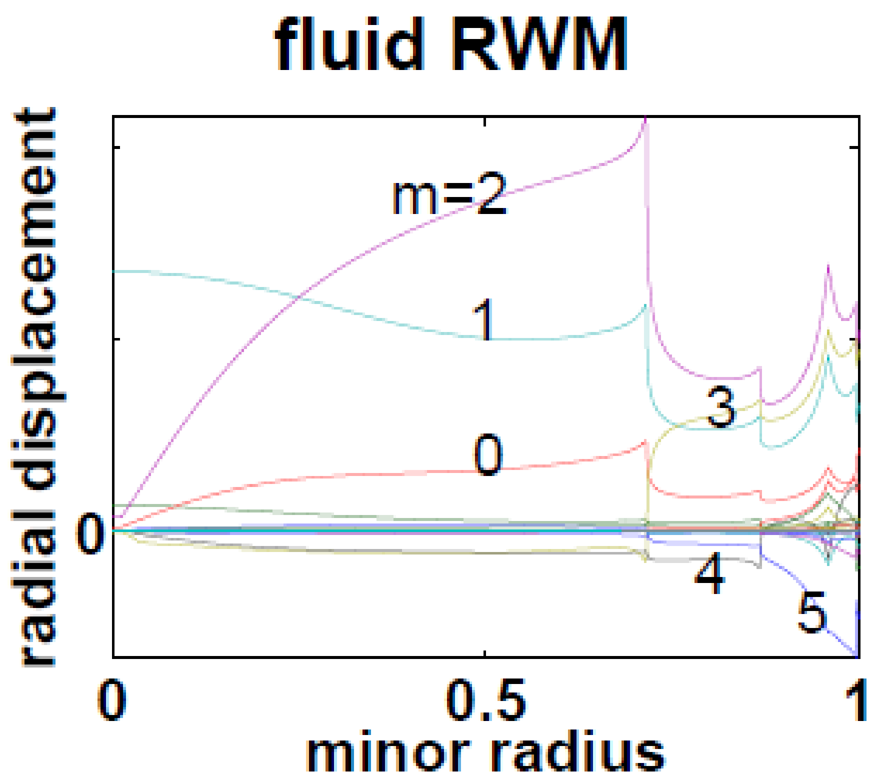

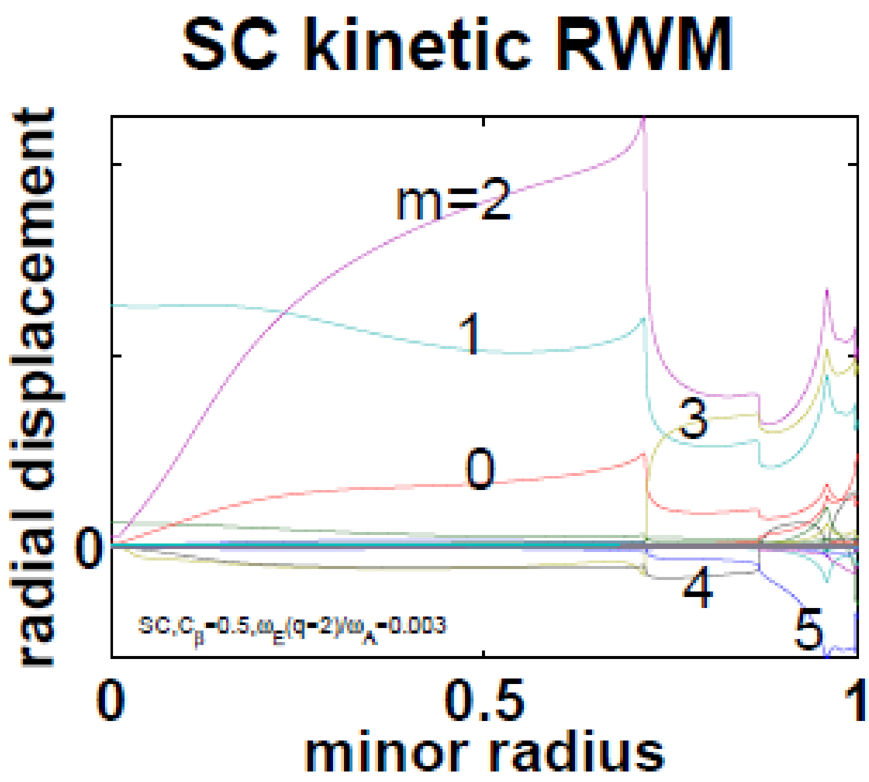

•*(Y. Liu, APS DPP 2008)*

Non-linear inclusion of γ and ω can be achieved in the perturbative approach through iteration

$$(\gamma - i\omega)\tau_w = -\frac{\delta W_\infty + \delta W_K}{\delta W_b + \delta W_K}$$

Example: NSTX 121083 @ 0.475

	τ_w = 0.1ms		τ_w = 0.5ms		τ_w = 1.0ms	
Iteration	γ	ω	γ	ω	γ	ω
0	-2577	-1576	-515	-315	-258	-158
1	-4906	431	-508	-172	-256	-139
2	-5619	800	-505	-177	-257	-140
3	-5745	828	-504	-179		
4	-5834	835				
5	-5855	838				
6	-5835	819				

The effect of iteration depends on the magnitudes of γ, ω

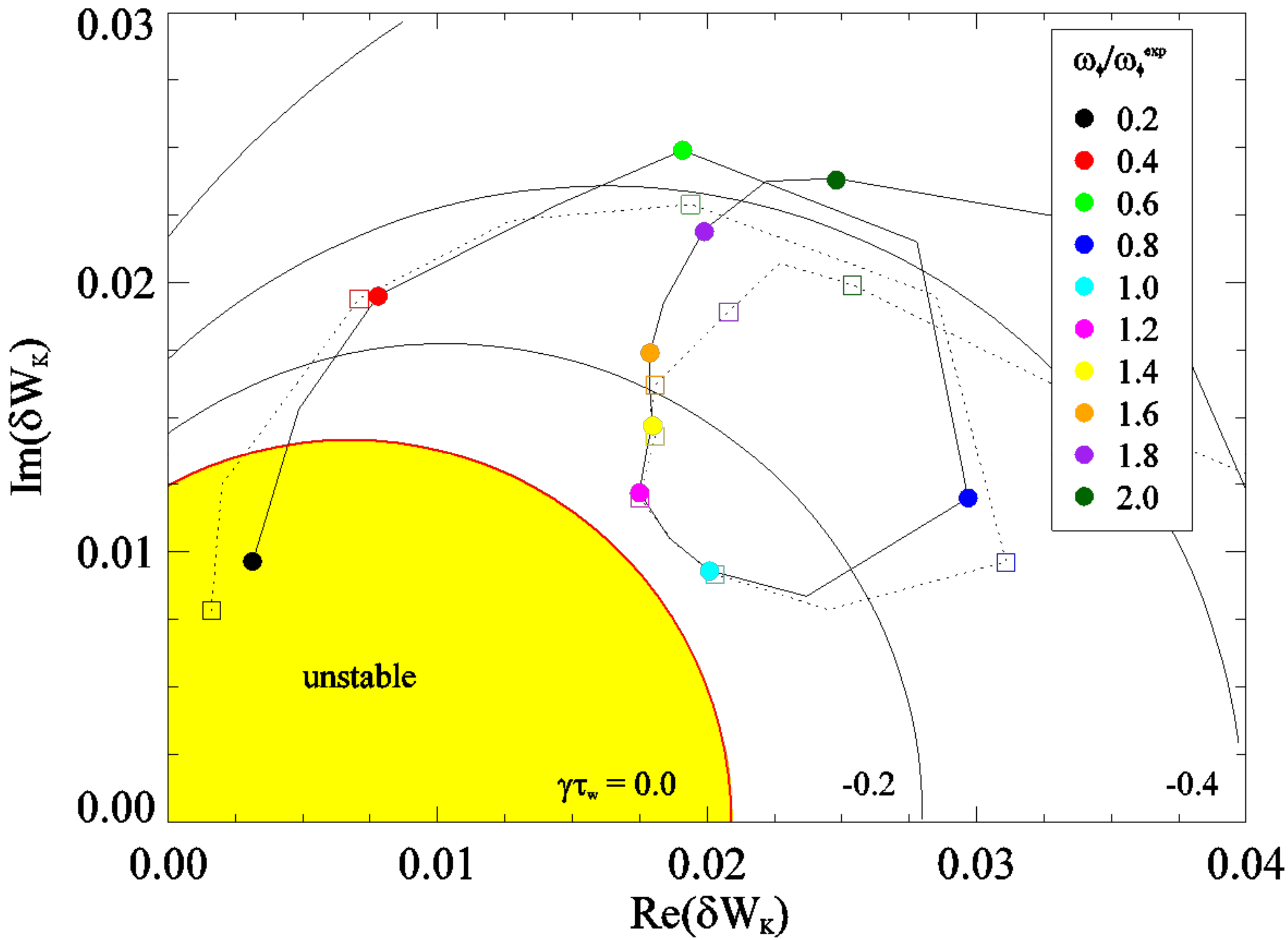

The dispersion relation has three roots

$$C = c_2 \int_0^\infty \left[\frac{\hat\omega_{*N} + (\hat\varepsilon - \frac{3}{2})\hat\omega_{*T} + \hat\omega_E + \hat\omega - i\hat\gamma}{\hat\omega_D \hat\varepsilon^a + \hat\omega_E + \hat\omega - i\hat\gamma} + \frac{-\hat\omega_{*N} - (\hat\varepsilon - \frac{3}{2})\hat\omega_{*T} + \hat\omega_E + \hat\omega - i\hat\gamma}{-\hat\omega_D \hat\varepsilon^a + \hat\omega_E + \hat\omega - i\hat\gamma} \right] \hat\varepsilon^{\frac{5}{2}} e^{-\hat\varepsilon} d\hat\varepsilon$$

Liu's simple example: a=0, c_2 = 0.18, ω_{*T} = 0

$$D = (\hat\gamma + i\hat\omega)(\hat\gamma_f^{-1} + C) - 1 + C$$

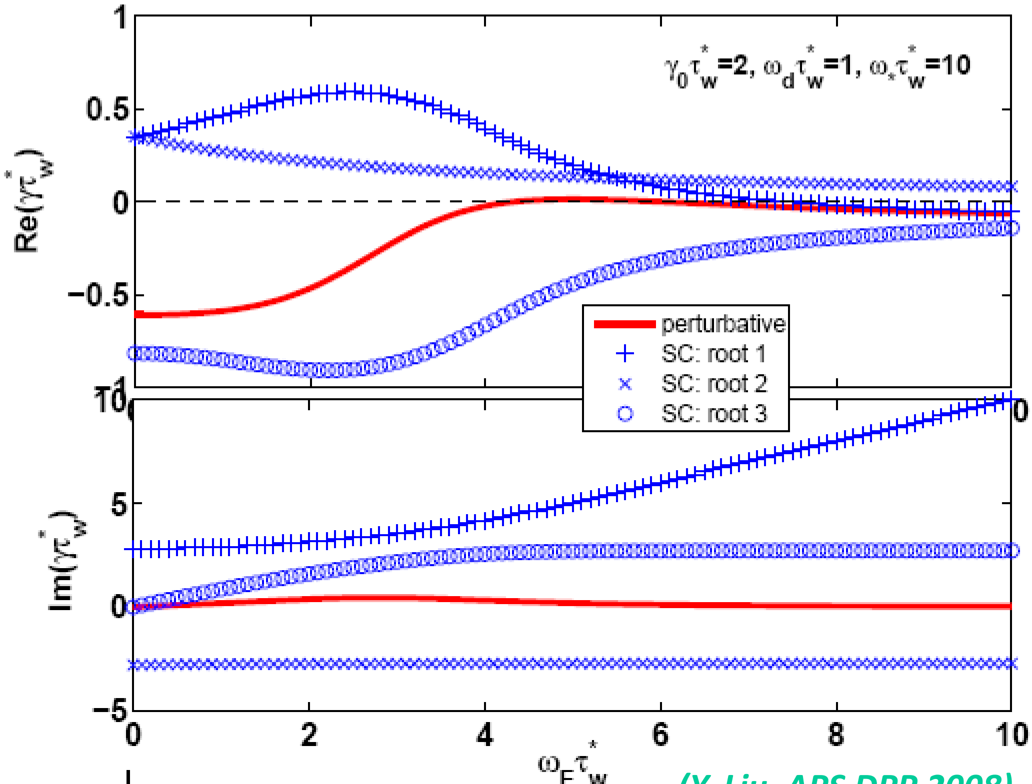

(Y. Liu, APS DPP 2008)

Plot contours of 1/|D|

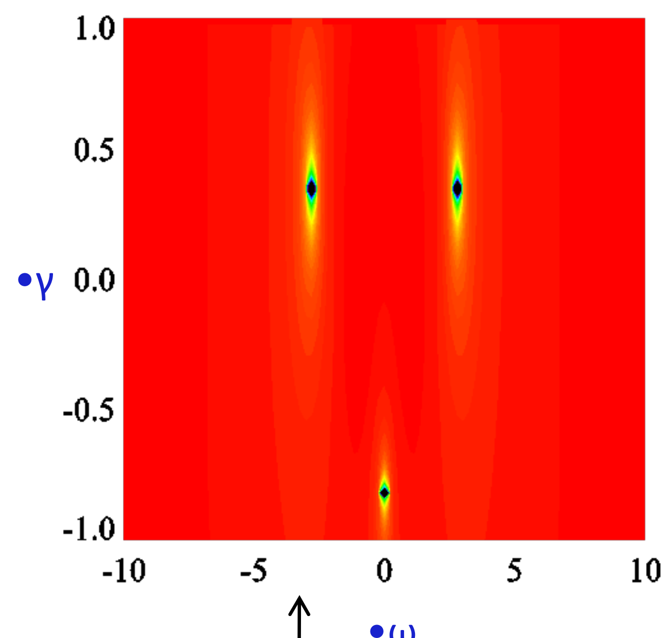

MISK and MARS-K Benchmarking

MISK and MARS-K were benchmarked using a Solov'ev equilibrium

$$\mu_0 P(\psi) = -\frac{1+\kappa^2}{\kappa R_0^3 q_0}\psi, \quad F(\psi) = 1$$

$$\psi = \frac{\kappa}{2R_0^3 q_0}\left[\frac{R^2 Z^2}{\kappa^2} + \frac{1}{4}\left(R^2 - R_0^2\right)^2 - a^2 R_0^2\right]$$

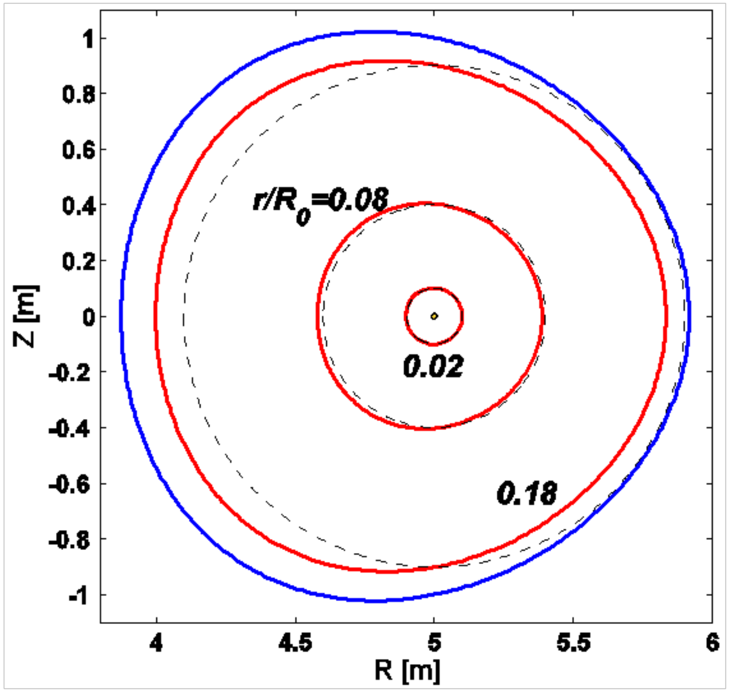

(Liu, ITPA MHD TG Meeting, Feb. 25-29, 2008)

- Simple, analytical solution to the Grad-Shafranov equation.
- Flat density profile means $\omega_{*N} = 0$.
- Also, ω, γ, and ν_{eff} are taken to be zero for this comparison, so the frequency resonance term is simply:

$$\delta W_K \propto \int \left[\frac{\left(\hat{\varepsilon} - \frac{3}{2}\right)\omega_{*T} + \omega_E}{\langle \omega_D \rangle + l\omega_b + \omega_E}\right] \hat{\varepsilon}^{\frac{5}{2}} e^{-\hat{\varepsilon}} d\hat{\varepsilon}$$

MARS-K: *(Liu, Phys. Plasmas, 2008)*

Drift frequency calculations match for MISK and MARS-K

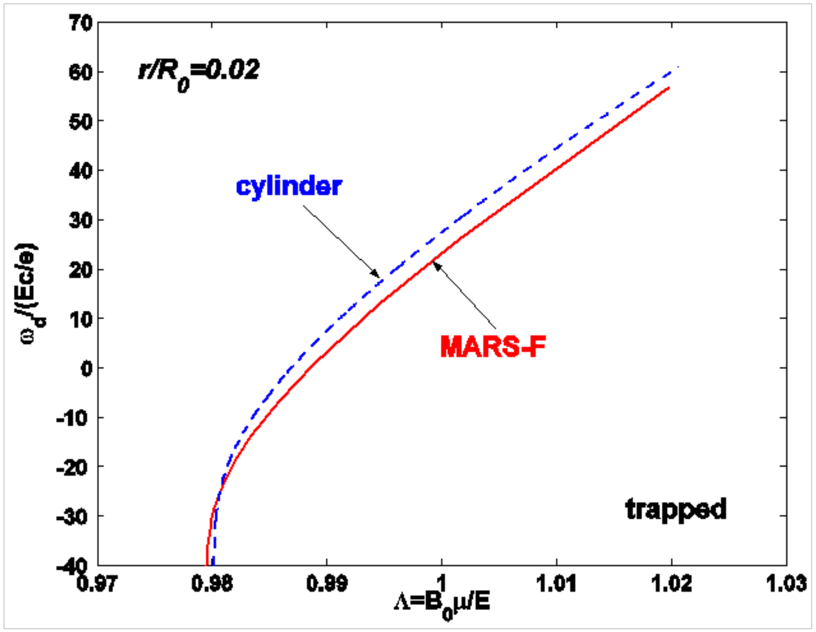

MARS

(Liu, ITPA MHD TG Meeting, Feb. 25-29, 2008)

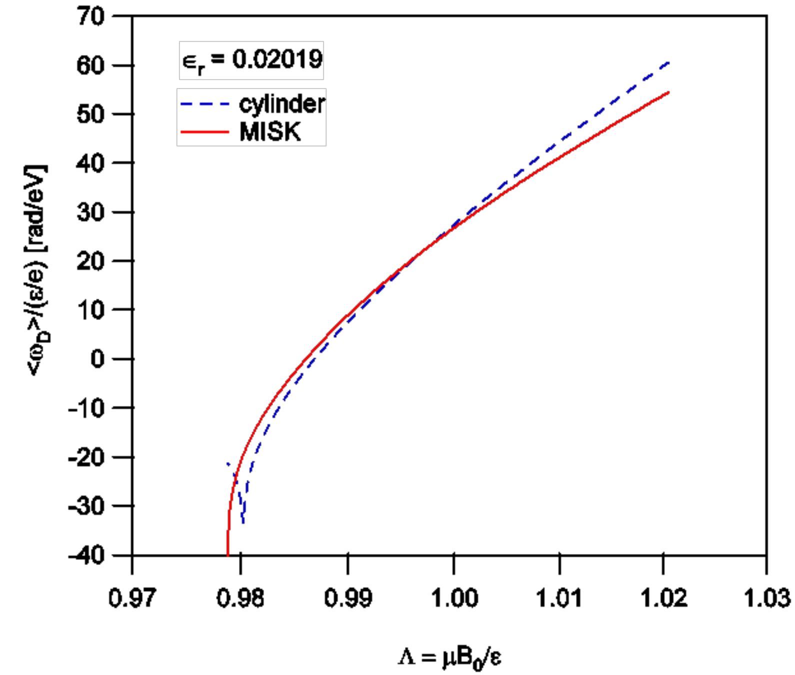

MISK

large aspect ratio approximation *(Jucker et al., PPCF, 2008)*

$$\frac{\langle \omega_D \rangle}{\varepsilon / e} = \frac{2q\Lambda}{R_0^2 B_0 \epsilon_r}\left[(2s+1)\frac{E\left(k^2\right)}{K\left(k^2\right)} + 2s\left(k^2 - 1\right) - \frac{1}{2}\right] \qquad k = \left[\frac{1 - \Lambda + \epsilon_r \Lambda}{2\epsilon_r \Lambda}\right]^{\frac{1}{2}}$$

here, ϵ_r is the inverse aspect ratio, s is the magnetic shear, K and E are the complete elliptic integrals of the first and second kind, and $\Lambda = \mu B_0/\varepsilon$, where μ is the magnetic moment and ε is the kinetic energy.

Bounce frequency calculations match for MISK and MARS-K

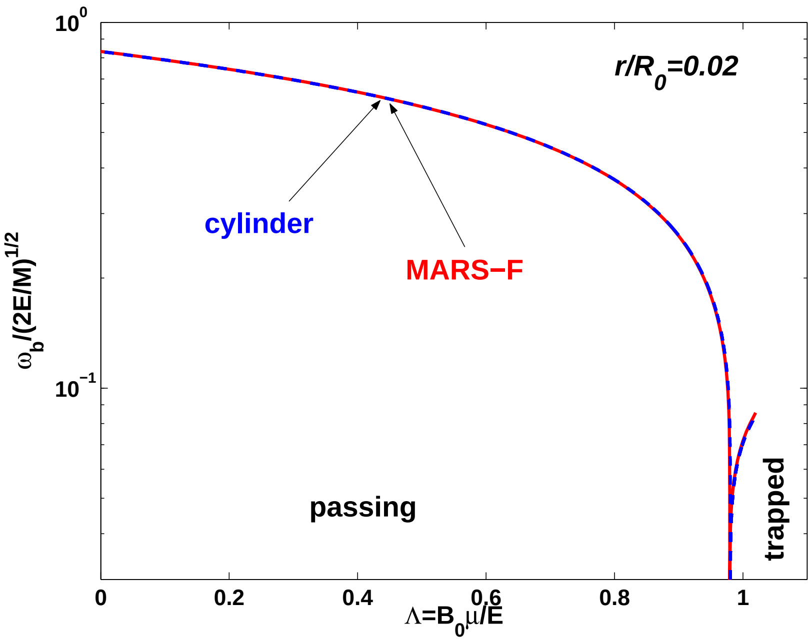

MARS

(Liu, ITPA MHD TG Meeting, Feb. 25-29, 2008)

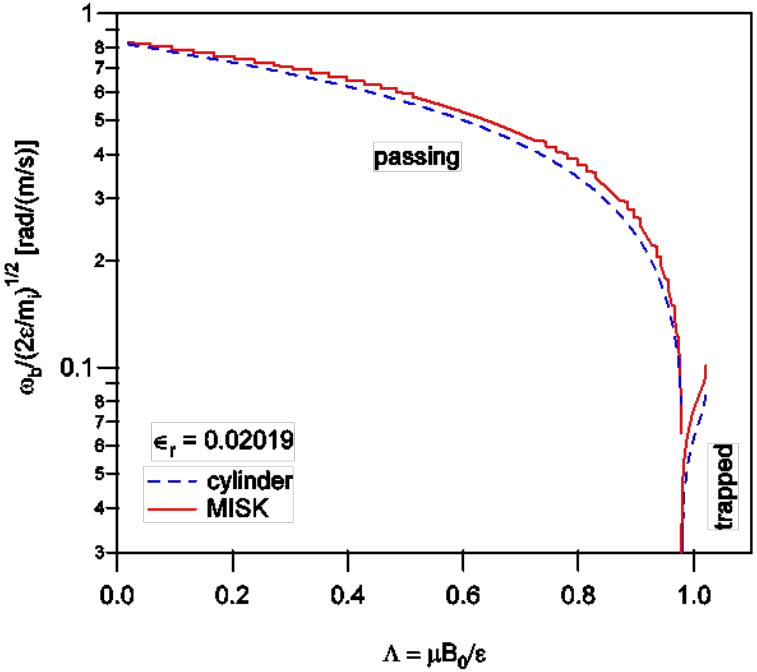

MISK

large aspect ratio approximation *(Bondeson and Chu, PoP, 1996)*

$$\frac{\omega_b}{\sqrt{2\varepsilon/m_i}} = \frac{\sqrt{2\epsilon_r\Lambda}}{4qR_0}\frac{\pi}{K(k)} \quad \text{(trapped)} \qquad \frac{\omega_b}{\sqrt{2\varepsilon/m_i}} = \frac{\sqrt{1-\Lambda+\epsilon_r\Lambda}}{2qR_0}\frac{\pi}{K(1/k)} \quad \text{(circulating)}$$

$$k = \left[\frac{1-\Lambda+\epsilon_r\Lambda}{2\epsilon_r\Lambda}\right]^{\frac{1}{2}}$$

MISK and MARS-K match well at reasonable rotation

Good match for trapped ions and electrons at high rotation, but poor at low rotation.

The simple frequency resonance term denominator causes numerical integration problems with MISK that don't happen with realistic equilibria.

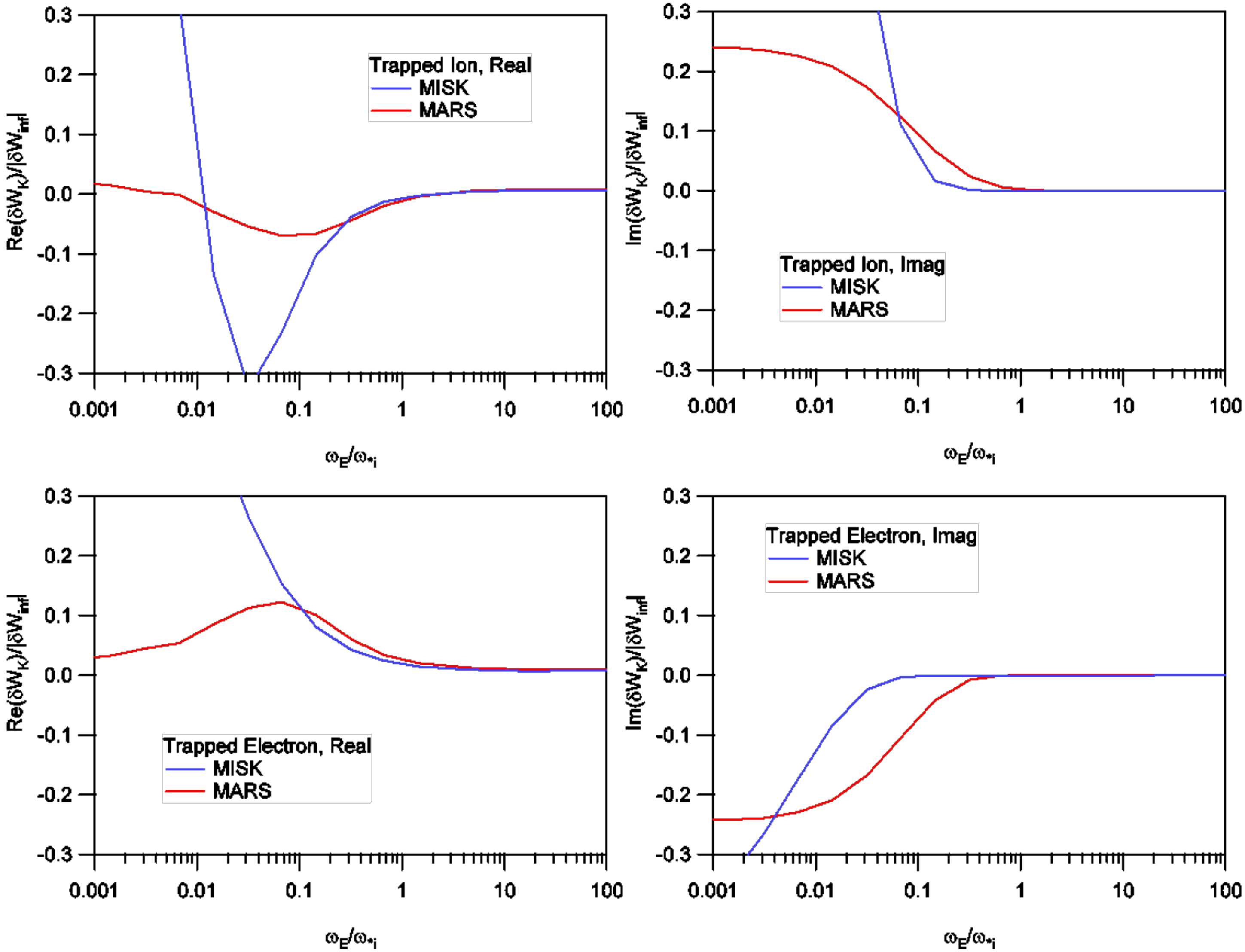

DIII-D Energetic Particle Experiment

MISK calculations indicate importance of energetic ions for RWM stability in low rotation DIII-D plasmas

[D3D MP 2009-99-07 by Reimerdes, Berkery, et al.]

- **Kinetic calculations using thermal particles only predict RWM to be most unstable at finite rotation**
  - Resonance with **precession frequency** of trapped particles at lower rotation
  - Resonance with **bounce frequency** of trapped particles at higher rotation
  - → RWM least stable for profile with $\Omega\tau_A$~1% at q=2

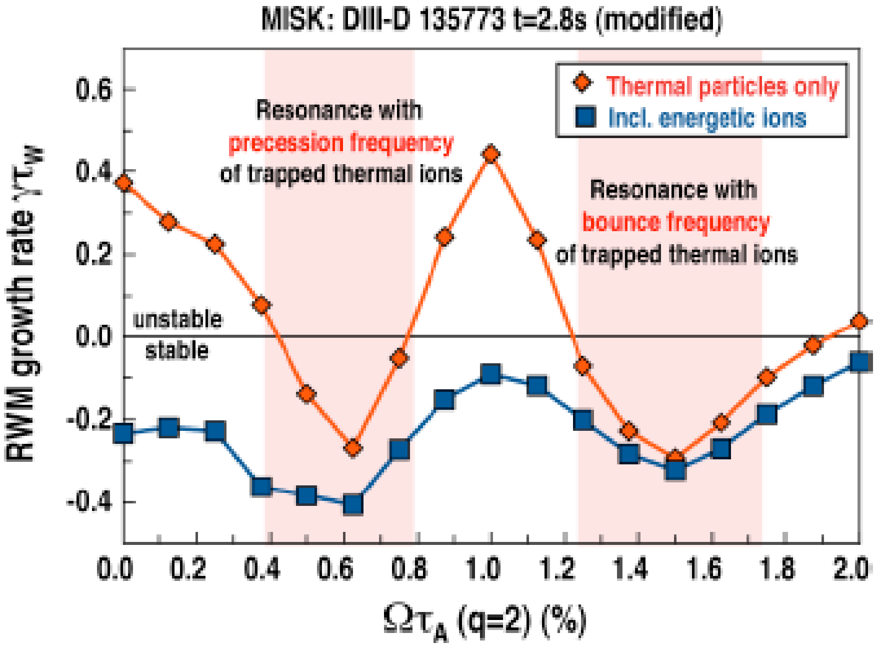

- **Trapped energetic ions (W_{fast}/W_{tot} ~23%) predicted to stabilize the equilibrium across the entire (low) rotation range**
  - Rotation dependence smeared out by resonance with precession frequency with trapped energetic ions
  - Low rotation wall stabilized plasmas typically have W_{fast}/W_{tot}>30%

Recent experiment tests kinetic stability models by reducing the energetic ion content

[D3D MP 2009-99-07 by Reimerdes, Berkery, et al.]

- An exploratory experiment succeeded in lowering W_{fast}/W_{tot} from ~35% to ~20%
  - Higher density
  - Higher plasma current
- RWM remains stable but an increased plasma response to applied n=1 field indicates weaker stabilization at lower plasma rotation Ω

→ Further experiments should look for a maximum in the amplification at finite rotation

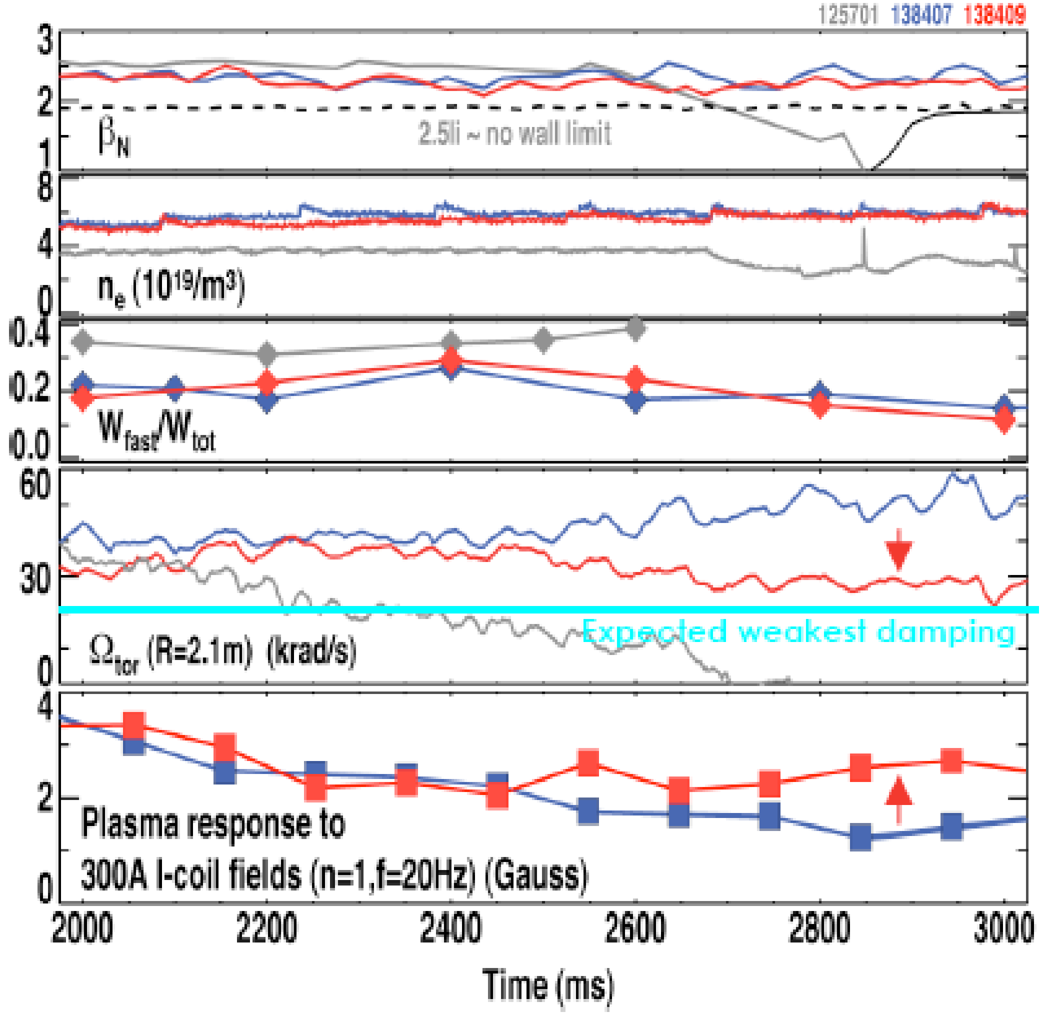

δW_K in the limit of high particle energy

Writing δW_K without specifying *f*:

$$\delta W_K = -\sqrt{2}\pi^2 \sum_{\pm\sigma} \sum_{l=-\infty}^{\infty} \int d\varepsilon \int d\Lambda \int d\Psi m^{-\frac{3}{2}} \frac{\hat{\tau}}{B_0} \frac{(\omega_r + i\gamma)\frac{\partial f}{\partial \varepsilon} + \frac{\partial f}{\partial \Psi}}{\langle \omega_D \rangle + l\omega_b - i\nu_{\rm eff} + \omega_E - \omega_r - i\gamma} \varepsilon^{\frac{5}{2}} \left| \langle HT/\varepsilon \rangle \right|^2$$

Rewriting with explicit energy dependence:

$$\delta W_K = -\sqrt{2}\pi^2 \sum_{\pm\sigma} \sum_{l=-\infty}^{\infty} \int d\varepsilon \int d\Lambda \int d\Psi m^{-\frac{3}{2}} \frac{\hat{\tau}}{B_0} \frac{(\omega_r + i\gamma)\frac{\partial f}{\partial \varepsilon} + \frac{\partial f}{\partial \Psi}}{\varepsilon \overline{\langle \omega_D \rangle} + l\sqrt{\varepsilon}\,\overline{\omega_b} - i\varepsilon^{-\frac{3}{2}}\overline{\nu_{\rm eff}} + \omega_E - \omega_r - i\gamma} \varepsilon^{\frac{5}{2}} \left| \langle HT/\varepsilon \rangle \right|^2$$

So that, for energetic particles, where ε is very large:

large

$$\delta W_K = -\sqrt{2}\pi^2 \sum_{\pm\sigma} \sum_{l=-\infty}^{\infty} \int d\varepsilon \int d\Lambda \int d\Psi m^{-\frac{3}{2}} \frac{\hat{\tau}}{B_0} \frac{(\omega_r + i\gamma)\frac{\partial f}{\partial \varepsilon} + \frac{\partial f}{\partial \Psi}}{\varepsilon \overline{\langle \omega_D \rangle} + l\sqrt{\varepsilon}\,\overline{\omega_b} - i\varepsilon^{-\frac{3}{2}}\overline{\nu_{\rm eff}} + \omega_E - \omega_r - i\gamma} \varepsilon^{\frac{5}{2}} \underbrace{\left| \langle HT/\varepsilon \rangle \right|^2}_{\text{Note: this term is independent of } \varepsilon.}$$

large large

XXX